NACA RM E55K25

c2

NACA

RESEARCH MEMORANDUM

INVESTIGATION OF AFTERBURNER COMBUSTION SCREECH AND METHODS OF ITS CONTROL AT HIGH COMBUSTOR PRESSURE LEVELS

By Arthur M. Trout, William K. Koffel, and George R. Smolak

Lewis Flight Propulsion Laboratory
Cleveland, Ohio

NATIONAL ADVISORY COMMITTEE
FOR AERONAUTICS

WASHINGTON

May 14, 1956

NACA RM E55K25

NATIONAL ADVISORY COMMITTEE FOR AERONAUTICS

RESEARCH MEMORANDUM

INVESTIGATION OF AFTERBURNER COMBUSTION SCREECH AND METHODS OF ITS CONTROL AT HIGH COMBUSTOR PRESSURE LEVELS

By Arthur M. Trout, William K. Koffel, and George R. Smolak

SUMMARY

Various methods for the control of afterburner combustion screech at afterburner-inlet total pressures of from 4000 to 6400 pounds per square foot absolute were investigated experimentally. In general, the range of afterburner fuel-air ratios in which screech occurred and the intensity of screech did not vary appreciably in the range of pressures covered. However, several configurations which had mild screech tendencies at the lower pressures were screech-free, or nearly so, at higher pressure levels.

Screech was successfully eliminated over the range of pressures and fuel-air ratios investigated by several devices including a 20-inch length of corrugated louvered liner at the afterburner wall, a 7-inch perforated shroud around the outer ring of a 2-ring V-gutter flameholder, and a 2-ring V-gutter flameholder fabricated from perforated sheet metal. A 20-inch length of cylindrical liner spaced 5/8 inch from the afterburner wall and perforated with 3/16-inch-diameter holes on 1/2-inch centers did not entirely eliminate screech, but a 36-inch length of the same material did.

INTRODUCTION

The development of high-performance afterburners and ram jets has increased the instances and the intensity of combustion screech. The onset of screech has been reported to induce a high order of mixing and intensify the rate of flame propagation, often causing marked increases in combustion efficiency. With screech, heat-transfer rates and temperatures of the combustor parts increase greatly. ' Moderate to severe screech can cause rapid deterioration or failure of the flameholder and combustor shell. An understanding of screech phenomena is essential to the design of screech-free combustors or to the design of devices for control or elimination of screech in existing combustors.

Numerous investigations have been made into the nature of screech and its elimination (e.g., refs. 1 to 12). Phase measurements of the predominant screech frequencies observed in a number of burners correspond to simple modes of transverse oscillations in the burner chambers (refs. 2, 5, 7, and 11). The initiation and generation of screech depend on flow and combustion phenomena. However, the exact nature of this dependence has not been completely established. From speculation on the mechanism of screech, a number of theories have been evolved that are discussed in more detail in the references. In general, the theories are based on some phase of combustion kinetics, aerodynamics, acoustical resonance, or combinations such as combustion kinetics and acoustical resonance (ref. 2) and aerodynamics and combustion kinetics (refs. 1, 7, and 11).

The NACA Lewis laboratory has investigated many of these possibilities, both analytically and experimentally. Both small- and full-scale combustors were experimentally investigated at combustor-inlet total pressures of about 650 to 4200 pounds per square foot absolute. These investigations generally show that the intensity of screech and the range of fuel-air ratios over which screech is encountered increase as inlet total pressure increases. Wide gutters are also more prone to screech than narrow gutters under similar conditions (ref. 9). Screech was completely eliminated by a perforated acoustic-absorption liner (ref. 5). Whether these tendencies would continue at higher inlet pressures encountered during high-speed flight near sea level was unknown.

The purpose of the present investigation is to explore screech tendencies of various combinations of flameholder, combustor liner, and fuel-spray bars at combustor-inlet total pressures between 2 and 3 atmospheres. The objectives were (1) to see if the screech tendencies were similar to those observed at lower pressure levels, (2) to determine whether a perforated liner could prevent screech at high pressures, (3) to find critical dimensions of flameholders or liners that can prevent screech at high pressures, and (4) to investigate the influence of changes in aerodynamic flow on screech tendency.

In studying the effect of changing aerodynamic flow on screech, several flameholders were built with perforated gutters for the purpose of reducing the tendency for the formation and alternate shedding of large vortices from the gutter trailing edges. Such vortices are believed by some investigators (refs. 1, 7, and 11) to be the initiating or the sustaining mechanism of screech. Another family of flameholders was made with cylindrical shrouds around the outside gutter of conventional ring-type V-gutter flameholders. The shrouds were either solid or perforated. Their purpose was to inhibit screech by eliminating the shedding of large vortices and to forestall the coupling of transverse pressure oscillations with the combustion process taking place in the recirculating wake of the gutter.

The investigation was run on an afterburner connected to an axial-flow turbojet engine and covered simulated sea-level ram pressure ratios of 1.0 to 1.8 (flight Mach numbers of 0 to 0.96). This condition resulted in afterburner-inlet total pressures of 4000 to 6400 pounds per square foot absolute at rated engine speed and a turbine-discharge temperature of 1675° R. Afterburner fuel-air ratio was varied over as wide a range as possible for each configuration (i.e., from lean blow-out to wide-open position of the variable-area exhaust nozzle), except where severe-intensity screech was encountered.

APPARATUS

Engine and Afterburner

The engine used in the investigation was an axial-flow turbojet engine and afterburner combination equipped with a variable-area clamshell-type exhaust nozzle (fig. 1). Rated (military) performance for this engine at NACA standard sea-level conditions is 5425 pounds thrust at 7950 rpm, an inlet-air flow of 102 pounds per second, and a turbine-discharge temperature of 1725° R. Maximum thrust is 7500 pounds with afterburning.

The over-all length of the afterburner (fig. 2) including diffuser, combustion chamber, and exhaust nozzle is 112 inches. The diameter of the afterburner combustion chamber is 32.6 inches at the flameholder. The exhaust-nozzle area is approximately 1.94 square feet in the closed position and 3.33 square feet in the full-open position.

Installation

The engine with afterburner was installed on a thrust-measuring test stand. Air was supplied to the engine inlet from the laboratory supply system, and the exhaust gases discharged into an acoustical muffler at atmospheric pressure.

Afterburner Configurations

During the investigation 25 afterburner configurations were used. These configurations were produced through alterations to the fuel-spray bars, cooling system, flameholder, and liner. The combination of alterations used to make up each of the configurations is summarized in table I. Details of modifications to the various components are described in the following paragraphs.

[redacted]

Fuel-spray bars. - The afterburner used in this investigation was originally designed for moderate thrust increases and was equipped with two identical sets of relatively short spray-bar fuel injectors in the turbine-discharge annulus, each set having 19 spray bars. The upstream and downstream sets were located 29.5 and 26.5 inches, respectively, upstream of the flameholder (fig. 2). The circumferential location was identical for both sets of bars and is shown in figure 3(a). Figure 3(b) shows the hole locations for the original spray bars, which are hereinafter referred to as the "short" fuel bars. These short bars were used only in configurations 1 and 3.

In order to permit afterburner operation for the screech investigation at good efficiency and at as high a temperature as would be permitted by the exhaust-nozzle maximum area, another set of bars was used which provided a more uniform radial fuel distribution than the short set. Details of these bars, hereinafter referred to as the "long" fuel bars, are shown in figure 3(c).

Fuel flow to the upstream and downstream fuel-bar manifolds was controlled automatically by a fuel-flow divider mounted on the engine. All bars sprayed fuel normal to the gas stream.

The engine and afterburner fuel used throughout the investigation conformed to the specification MIL-F-5624B, grade JP-5, having a lower heating value of 18,625 Btu per pound and a hydrogen-carbon ratio of 0.159.

Cooling systems. - The original afterburner design provided for cooling of the combustion-chamber wall by the flow of turbine-discharge gas behind a corrugated and louvered cooling liner that extended from the flameholder to the exhaust-nozzle inlet. The exhaust nozzle was cooled by ducting compressor bleed air through the double walls of the stationary part of the exhaust nozzle (fig. 2).

In order to cool the afterburner adequately with the liner removed and with the more uniform fuel pattern (which increased the gas temperature near the wall), a modified cooling system was employed. The combustion-chamber wall was cooled by means of an external sheet-metal shroud extending from the flameholder region to the double-walled exhaust-nozzle section (fig. 2). Air from the laboratory system was supplied at ambient temperature to four locations around the cooling-shroud manifold. In addition, the modified cooling system used water instead of air to cool the exhaust nozzle.

Flameholders. - Flameholder A (fig. 4(a)) was a conventional 2-ring V-gutter design that blocked 27 percent of the combustion-chamber cross-sectional area. The gutter width was $1\frac{1}{2}$ inches. Two slightly different

support structures for this flameholder were used during the investigation, but the differences were considered inconsequential.

Flameholder B1 (fig. 4(b)) had four annular V-gutters, 3/4 inch wide. Blockage was 25 percent. Flameholder B2 (fig. 4(c)) had two annular V-gutters, 3/4 inch wide. Blockage was 15 percent.

Type C flameholders were made by attaching various shrouds to a type A flameholder. The shroud details are shown in figure 4(d). The increase in flameholder blockage due to the addition of the shrouds was negligible.

Flameholder D1 (fig. 4(e)) was a single annular V-ring, 3 inches wide and 7 inches deep with a rounded apex. Blockage was 27 percent. Flameholders D2 and D3 were identical to D1, except that flameholder D2 was perforated with 1/2-inch-diameter holes as shown in figure 4(e), and flameholder D3 had an all-over perforation pattern of 3/16-inch holes on 1/2-inch centers. Flameholder D4 (fig. 4(f)) was similar to flameholder A, except that the depth of the annular V-gutter was increased from 2 to 4 inches, and the entire flameholder was perforated with 3/16-inch holes on 1/2-inch centers. Except for the holes, the blockage was the same as for flameholder A.

Flameholder E (fig. 4(g)) was made by attaching a 3.25-inch-wide annular piece of 4-mesh 0.090-diameter wire screen to the outer gutter of a type A flameholder. The screen extended from the apex of the outer gutter to the afterburner wall. Blockage was 48 percent.

Combustor liners. - There were two types of liner material used in the investigation. Figure 5(a) is a photograph of the corrugated, louvered liner material, which is 1/32 inch thick and has a ceramic coating to reduce corrosion. Dimensions and locations of the corrugated liners are given in figure 5(c) to (f). (Liner L3 was made of the corrugated material but had the louvers welded shut.) Figure 5(b) is a photograph of the noncorrugated perforated liner material, which was 1/16-inch-thick Inconel perforated with 3/16-inch holes on 1/2-inch centers. The noncorrugated liners (fig. 5(g) and (h)) were spaced 5/8 inch from the burner wall.

Instrumentation

Instrumentation for the measurement of pressures and temperatures was installed at various stations in the engine and afterburner as indicated in figure 1. Engine air flow was measured at station 1 by means of a survery of total and static pressures and temperature. Afterburner-inlet conditions of temperature and pressure were measured at the turbine discharge, station 5. A survey of total pressures was made by means of a water-cooled rake at the entrance to the exhaust nozzle, station 9.

At station 6 provision was made for a fuel-air-ratio survey just ahead of the flameholder. Three different probe positions were used, one on top center of the burner and one $22\frac{1}{2}^{\circ}$ to each side of top center in the same circumferential plane. Fuel flows to the engine and to the afterburner were measured by calibrated, rotating-vane electronic flowmeters. Thrust was measured by a self-balancing null-type pneumatic thrust cell.

Screech was detected and identified by means of (1) auditory observations in the control room, (2) a microphone in the test cell used in conjunction with a magnetic tape recorder, (3) a pressure pickup mounted on the afterburner used in conjunction with a panoramic sonic analyzer, (4) frequency comparison with an audio oscillator. Also, the presence of screech, a rough indication of its intensity, and the location of maximum pressure fluctuations were indicated on U-tube manometers connected to pairs of differential pressure orifices (fig. 6). Four groups, each containing 10 pairs of orifices, were located in the 24 inches of burner wall just downstream of the flameholder. Manometer-board capacity permitted only six pairs per group to be connected at one time. The principle of operation of the differential orifices is that the flow coefficient of a tapered orifice differs for flow in one direction from that for flow in the opposite direction. When two orifices connected to a U-tube manometer are oriented as shown in figure 6(c) and put into a fluctuating pressure field, gases are trapped in one leg of the system because when a compression wave hits the orifices more fluid enters one orifice than the other, and during the following rarefaction, when the flow through the orifices reverses direction, the orifice which passed more fluid during the pressure wave will lose less than the other. As this cycle is repeated, a considerable pressure differential can be built up, the higher pressure being in the leg with the sharp edge facing away from the zone of fluctuating pressure. No attempt was made to calibrate the orifice pairs to make them suitable for obtaining a quantitative measure of pressure fluctuations.

PROCEDURE

Simulated Flight Conditions

All tests were made with the engine exhausting to atmospheric pressure. The pressure at the engine inlet was varied to cover a range of simulated sea-level flight Mach numbers of from 0 to 0.96 (engine ram ratios of 1.0 to 1.8). In order to attain the highest afterburner pressures practicable without unduly stressing the compressor casing, the inlet air was taken directly from the laboratory supply system and was not preheated to simulate actual flight conditions. Inasmuch as the air-supply temperature was in the range of 40° to 70° F, a ram ratio of only

1.45 to 1.53 was needed to simulate the turbine-discharge pressure corresponding to an actual ram ratio of 1.8 with the correct sea-level ram temperature of 155° F at the inlet. This is true because the lower inlet temperature permits the compressor to operate at a higher corrected speed (and pressure ratio) while the turbine pressure ratio remains constant.

Turbine-discharge temperature for this investigation was maintained at approximately 1675° R at an actual engine speed of 7950 rpm.

Afterburner Operation

In general, the following sequence of operation was followed:

(1) The engine-inlet pressure was set for a sea-level ram ratio of 1.0.

(2) The afterburner was lighted near the lean blow-out fuel setting. (No special ignition source was used, inasmuch as autoignition of the afterburner occurred at all operating conditions as soon as sufficient fuel was introduced to maintain afterburning.)

(3) If there was no screech, the afterburner fuel-air ratio was increased from the region of lean blow-out until screech was encountered or the adjustable nozzle was fully open.

(4) The ram pressure ratio was increased in steps up to a simulated value of 1.8, repeating step (3) at each new pressure.

(5) Whenever possible, the boundary between screeching and screech-free operation was noted and the principal screech frequency measured.

RESULTS AND DISCUSSION

A graphical summary of the results of this investigation is shown in figure 7. This series of bar charts shows the operational characteristics for the various configurations and will be referred to as each configuration appears in the subsequent discussion.

General Afterburner Performance Characteristics

with Short and Long Fuel Bars

The performance of the original afterburner (configuration 1) is shown in figure 8, and the operational characteristics in figure 7(a).

Afterburner combustion efficiency is defined herein as the ratio of actual to ideal temperature rise in the afterburner. Afterburner-exit temperature was calculated from engine air flow, thrust, and nozzle pressure ratio. Afterburner fuel-air ratio is based on unburned air entering the afterburner except where noted. Configuration 1 had the short set of fuel-spray bars, the 48-inch corrugated louvered liner L1 (fig. 5(c)), and the 2-ring $1\frac{1}{2}$-inch-wide V-gutter flameholder A (fig. 4(a)). No screeching combustion was observed for this configuration over the range of operating conditions investigated. The peak afterburner combustion efficiency is shown in figure 8(a) to be 0.87 at an afterburner fuel-air ratio of about 0.03.

Data are shown for the lowest and highest pressure levels investigated. Average afterburner-inlet pressures for the data at ram ratios of 1.0 and 1.8 were 4200 and 6300 pounds per square foot absolute, respectively. Combustion efficiency was essentially the same for both pressure levels. Also indicated in figure 8(a) are the limits of operation of the afterburner at ram ratios of 1.0 and 1.8 when the production engine control system was used. Most of the investigation was conducted by overriding the control. The decrease in afterburner combustion efficiency at higher fuel-air ratios (when overriding the control) was to be expected, because this configuration was originally designed for only moderate augmentation ratios. The afterburner total-pressure-loss ratio (fig. 8(b)) varied from 0.06 with no afterburning to 0.088 at an afterburner fuel-air ratio of 0.067.

Figure 8(c) is a contour map of fuel distribution constructed from the three radial surveys made in the annular area just ahead of the flameholder (station 6, fig. 1) for afterburner fuel-air ratios of 0.025 and 0.040. Figures given on the contours, however, are for total fuel-air ratio at this station rather than the afterburner fuel-air ratio, which is based on unburned air. The use of the relatively short fuel bars in this configuration resulted in an overrich region toward the center of the burner. This condition was also evidenced by visual observations made during afterburning. A rather well-defined core of luminous flame could be seen issuing from the nozzle, especially during operation at the higher fuel-air ratios. This overrich condition caused the combustion efficiency (fig. 8(a)) to decrease above a fuel-air ratio of 0.03.

Afterburner performance of configuration 2, which utilized the long set of fuel bars, is shown in figure 9, and operational characteristics in figure 7(a). In this configuration the original 48-inch corrugated and louvered liner was shortened to 20 inches (fig. 5(d)). No screech was encountered with this configuration. Peak afterburner combustion efficiency (fig. 9(a)) was close to 100 percent at an afterburner fuel-air ratio of about 0.04 and was insensitive to burner-inlet total pressure between 4050 and 6350 pounds per square foot absolute (average

burner-inlet total pressures for data points at ram ratios 1.0 and 1.8, respectively). Afterburner total-pressure loss (fig. 9(b)) was 0.06 for nonafterburning conditions and approached 0.10 at an afterburner fuel-air ratio of 0.05.

The more uniform fuel distribution of the long set of fuel bars may be seen by comparing the total-fuel air-ratio contour maps for configuration 2 shown in figure 9(c) with those from the short-bar configuration (fig. 8(c)). Both figures were constructed from similar surveys at the same afterburner fuel-air ratios. The more uniform fuel distribution raised the peak afterburner combustion efficiency about 13 percentage points and permitted operation at higher temperature levels. The maximum exhaust-nozzle area limited operation to afterburner fuel-air ratios of slightly under 0.05. Exhaust-gas temperature at wide-open exhaust nozzle was about 3600° R.

Effect of Screech on Combustion Efficiency

Near Lean Blow-Out

The configuration reported in figure 9 could be made to screech by shortening or removing the 20-inch corrugated louvered liner. Several data points taken near lean blow-out at a ram ratio of 1.0 during medium-intensity screech are shown in figure 9(a) by tailed symbols. The screech did not materially improve combustion efficiency at these conditions. This is probably to be expected in view of the good fuel pattern, long combustion chamber, and high pressure level. Screech would be more likely to increase combustion efficiency in a burner having poor fuel distribution (by improving mixing of overrich mixture with unburned air in the combustion zone) or short length (by increasing the heat release per unit volume in combustion zone due to rapid flame spreading). This negligible effect of screech on afterburner combustion efficiency was also noted for several other configurations.

Characteristics of Screech with 2-Ring V-gutter Flameholder and No Liner

Configuration 3 included the short set of spray bars, the 2-ring V-gutter flameholder, and no liner. At a ram ratio of 1.0, mild screech was observed from lean blow-out to an afterburner fuel-air ratio of 0.0525, at which point severe screech began (fig. 7(a)). As pressure level was increased, the lean fuel-air-ratio zone became screech-free; and at a ram ratio of 1.8 there was no screech from lean blow-out to an afterburner fuel-air ratio of 0.0525, at which point mild screech set in. The screech frequency for this configuration varied from about 1150 cps

near lean blow-out to nearly 1300 cps at the richest fuel-air ratios, as would be expected from the temperature change (ref. 6). This frequency corresponds to the first radial mode of oscillation as given in reference 6. According to theoretical considerations in references 2 and 12, the driving forces for this mode of oscillation would be favored by a high rate of heat release at the center of the burner such as would occur with the short spray bars.

With the long fuel bars (configuration 4), a medium-intensity screech of about 540 cycles was observed from lean blow-out to an afterburner fuel-air ratio of about 0.037 at a ram ratio of 1.0 (fig. 7(a)). This screech frequency corresponds to the first transverse mode of oscillation as described in reference 6. According to references 2 and 12, the driving forces for the transverse modes would be favored by heat release toward the outer wall of the burner. The more uniform fuel distribution provided by the long spray bars evidently facilitated oscillation in the first transverse mode. From a fuel-air ratio of 0.037 to wide-open exhaust nozzle, however, the principal screech frequency was about 1220 cps. Screech characteristics of configuration 4 were not investigated at higher ram ratios.

3943

Effect of Various Liners on Screech

One of the most common methods of eliminating screech has been the use of an acoustical liner near the combustor wall. These liners suppress screech by absorbing or breaking up pressure waves, thus preventing their reflection into the combustion zone and interrupting the screech cycle. In order to determine the effectiveness of screech-suppressing liners at high pressures, a number of different liner configurations were investigated.

As previously noted, the 20-inch length of corrugated louvered liner in configuration 2 was sufficient to eliminate screech at all conditions investigated. This same 20-inch liner was run with the single-ring flameholder D1 (fig. 4(e)) in configuration 5. This flameholder with its 3-inch-wide gutter would be expected to have very strong screech tendencies (refs. 5 and 6). The 20-inch liner prevented screech in configuration 5 over the full range of fuel-air ratios (fig. 7(a)).

Configuration 6 was similar to configuration 2 (which did not screech), except that the louvers in the 20-inch corrugated liner L3 were welded shut. This configuration had mild screech at intermediate afterburner fuel-air ratios (0.038 to 0.041, fig. 7(a)).

Screech was encountered when the 20-inch corrugated louvered liner of configuration 2 was shortened 5 inches at either the downstream end (configuration 7) or the upstream end (configuration 8)(fig. 7(a)).

The screech with configuration 8 was mild and occurred only at intermediate afterburner fuel-air ratios. As the pressure was increased, the screech zone shrank and the screech became progressively milder until it faded away completely at a ram ratio of 1.8.

Liner L6 of configuration 9 was a 20-inch length of noncorrugated metal perforated with 3/16-inch holes on 1/2-inch centers (fig. 5(g)). This length of liner did not eliminate screech except at rich afterburner fuel-air ratios at ram ratio 1.8 (fig. 7(a)). In configuration 10 the noncorrugated liner was lengthened to 36 inches, and screech was completely eliminated (fig. 7(a)). This effect of noncurrugated perforated liner length is similar to that found in the investigation at lower pressure levels reported in reference 5.

Comparison of the results for configurations 2 and 6 and configurations 2 and 9, shows that, for a screech-suppressing acoustical liner, both the corrugations and louvers (or perforations) are helpful, which is in agreement with the findings of reference 7. The corrugated and louvered liner would probably also be preferable to a cylindrical perforated liner with respect to cooling and structure.

Shrouded Flameholders with No Liner

Inasmuch as screech is intimately concerned with the combustion process, it seems logical that a screech eliminator might be most effective if located near a critical combustion zone. The results of flame-stabilization and propagation studies indicate that conditions in the region of the flameholder determine to a large extent the character of the combustion process. Therefore, a series of flameholders employing a perforated shroud spaced 1/2 inch from the outer gutter of the 2-ring, $1\frac{1}{2}$-inch-wide V-gutter flameholder was investigated. The purpose of these shrouds was to prevent the reflection of transverse pressure waves from the flame front to the combustor wall and back into the critical combustion zone where the flame is attached to the flameholder.

Configurations 11 and 12, respectively, had shroud lengths of 10 and 7 inches, of which $1\frac{1}{2}$ inches extended upstream of the trailing edge of the flameholder gutter (fig. 4(d)). Neither of these configurations screeched over the range of operable fuel-air ratios and pressures (fig. 7(b)). When the shroud was shortened to 4 inches (configuration 13), screech was observed in the region of operation near lean blow-out.

Removing the upstream $1\frac{1}{2}$-inch portion of the 4-inch shroud (configuration 14) increased the screech zone near lean blow-out but still

left a screech-free region of operation in the rich range of afterburner fuel-air ratios. A large hysteresis effect was noted for this configuration (especially at a ram ratio 1.0), as shown by the arrows in figure 7(b). As afterburner fuel was decreased from the screech-free rich zone, a mild 540-cycle screech set in at an afterburner fuel-air ratio of 0.034. When the afterburner fuel-air ratio was further reduced to 0.0305, severe 540-cycle screech set in, and it was then necessary to increase the fuel-air ratio to 0.037 before the screech stopped. Another characteristic of configuration 14 was that it was necessary to hold fuel flow constant for 3 to 4 seconds, compared with less than 1 second with most configurations, before screech would develop. No screech occurred at all if the afterburner fuel flow was increased or decreased at a moderate rate while passing through the screech zone.

In order to determine the effect of the perforations in the flameholder shroud, several lengths of solid shroud were investigated. The 4-inch solid shroud (configuration 15) had characteristics very similar to the $2\frac{1}{2}$-inch perforated shroud (fig. 7(b)), with screech occurring only in the lean region. The 7- and 10-inch lengths of solid shroud (configurations 16 and 17) screeched badly at all operating conditions investigated. During the run of the 10-inch solid shroud at ram ratio 1.8, the afterburner was severely damaged by a fatigue failure at a welded seam. The violent type of screech denoted by the darkest shading in figure 7(b) had no predominant audible frequencies. The panoramic sonic analyzer indicated this type of screech to be a complex combination of many frequencies. For configuration 15 there was almost a continuous band of oscillations in the frequency range of 400 to 2000 cycles, while for configuration 16 the band was from 1000 to 4000 cycles. The characteristic sound of this type of screech is a loud "hissing" noise rather than one or two discrete tones as in the more mild forms of screech observed.

Inasmuch as the 4-inch length of solid shroud, which had little if any sound-absorption capacity, was partially successful in eliminating screech, it is believed that acoustical absorption was not the essential factor. It may be that either the shroud was too close to the flame zone for any pressure waves to be reflected in such a manner as to excite a driving force commensurate with any transverse mode of oscillation, or else the shroud affected the aerodynamic flow of mixture past the flameholder in such a manner as to prevent the initiation of the screech cycle. The longer solid shrouds may have held flame themselves and thus moved the "critical zone" downstream to an unprotected region, or else the added length of solid material permitted the transverse screech waves to be reflected within the shrouds themselves.

In configuration 18 the 1/2-inch spacing between the perforated shroud of configuration 12 was eliminated, and the shroud was attached directly to the trailing edge of the outer gutter. The $1\frac{1}{2}$-inch portion of shroud extending upstream was discarded, thus leaving a $5\frac{1}{2}$-inch piece extending downstream of the flameholder. Configuration 18 screeched at all operating conditions (fig. 7(b)). No doubt the shroud attached directly to the outer gutter held flame, whereas the separated shroud probably did not; and the "critical zone" may thus have been moved downstream to an unprotected region at the end of the shroud.

Thus, it was demonstrated that 7- and 10-inch lengths of perforated shroud spaced 1/2 inch away from the outer gutter were successful in preventing screech at all conditions investigated, that shorter perforated shrouds and a 4-inch solid shroud were only successful in eliminating screech in the rich region, and that 7- and 10-inch lengths of solid shroud and a perforated shroud attached directly to the outer gutter screeched for all conditions of operation.

Perforated Flameholders

As previously mentioned in the INTRODUCTION, a number of investigators in the field of screeching combustion have concluded that screech is induced by a coupling of aerodynamic and combustion processes (refs. 1, 7, and 11) and that during screech the flow in the region of the flameholder is of a pulsating nature, which causes the shedding of large vortices from the flameholder. One method of approach to screech elimination would then be to alter the geometry of the flameholder or its environment so as to reduce the vortex-forming potential. As a result of an unreported investigation along these lines, it is claimed that screech in a particular afterburner was eliminated by perforating the flameholder gutters with holes. The hole configuration used was developed from a model investigation on a water table. The hole pattern was arranged so as to eliminate the large alternately shedding vortices in the wake of the flameholder model.

Smoke-tunnel investigation. - In order to determine the effectiveness of a perforated flameholder in preventing screech under the conditions of afterburning reported herein, a flameholder of similar cross section to the one in the aforementioned unreported investigation was fabricated and mounted on the flameholder base as shown in figure 4(e). A single-ring design was chosen in order to approximate the cross section of the original design (which had two very wide rings) and still keep the blockage in a reasonable range. Concurrently, an investigation was conducted in a low-velocity wind tunnel to determine perforation patterns that would eliminate the large alternating vortices which are shed in flameholder wakes under cold-flow conditions (ref. 13). The

test section of the tunnel used is shown in figure 10. Models with the same cross-sectional dimensions as the flameholder of figure 4(e) were mounted in the test section, and streams of smoke were introduced through probes on either side of the gutter to show the flow pattern in the wake of the model. Motion pictures at 64 frames per second were taken of the smoke trails in the wake of the unperforated-gutter model, and also of perforated-gutter models with various hole configurations. Tunnel velocity was maintained at a low level (maximum of about 6 ft/sec) while the movies were being taken, so that the smoke-trail density would be satisfactory for photographing. Visual observations made with high-intensity stroboscopic light at higher tunnel velocities (about 25 ft/sec) showed the wake patterns to be essentially the same as at the lower velocities.

Figure 11(a) is a movie sequence showing the typical wake pattern of the unperforated wide-gutter flameholder model. Figure 11(b) shows the wake of the same model after it had been perforated with the hole pattern shown in figure 4(e). This hole pattern was the most successful of a number of patterns tested in eliminating the two large alternately shedding vortices.

Flow-visualization studies were also made with several other flameholder models. Figure 11(c) shows the wake pattern of a model of the $1\frac{1}{2}$-inch-wide V-gutter of flameholder A, and figure 11(d) shows the pattern with a perforated shroud attached corresponding to the configuration of flameholder C2. It is interesting to note that the perforated shroud, which prevented screech during afterburning, also eliminated the large alternating vortices in the wake of the flameholder.

Operational characteristics in afterburner. - The solid wide-gutter flameholder (configuration 19) screeched badly at ram ratios of 1.0 and 1.8, as would be expected from previous experience which indicates that wide gutters are more prone to screech than the narrow gutters. As noted in figure 7(c), the rich region was not explored because of the violent character of the wide-frequency-band "hissing" type screech encountered with this configuration.

For configuration 20, the wide gutter was perforated with the hole pattern shown in figure 4(e), which was an outgrowth of the flow-visualization studies. This configuration showed a slight improvement over the solid flameholder in that the region of violent screech was smaller (fig. 7(c)). There was no screech in the rich region.

The perforation pattern for the wide-gutter flameholder of configuration 21 was 3/16-inch holes on 1/2-inch centers. This hole pattern was nearly as effective as that for configuration 20 in eliminating the large vortices in the flow-visualization studies. This configuration

did not screech in the lean region of operation but screeched badly in the rich region (fig. 7(c)). A hysteresis effect with the severe hissing screech was again noted.

Since the perforated wide gutters showed a slight improvement in screech characteristics over the solid wide gutter, it was thought that perhaps screech control with perforated gutters, though not a powerful screech remedy, might be more successful for a flameholder with weaker screech tendencies than the 3-inch-gutter flameholder. The 2-ring perforated flameholder D4 (fig. 4(f)) of configuration 22 had the same over-all dimensions as the original 2-ring, $1\frac{1}{2}$-inch-wide V-gutter flameholder A, except that the depth of the gutters was increased from 2 to 4 inches in order to preserve the general shape of the previous perforated flameholders. The hole pattern was 3/16-inch holes on 1/2-inch centers. This configuration did not screech at any operable fuel-air ratio (fig. 7(c)). The flameholder ran very hot and burned out in several places during the run at a ram ratio of 1.0; higher ram ratios were therefore not investigated. However, as will be discussed later, previous experience gained during this investigation indicated that this configuration probably would also have been screech-free at the higher pressure levels.

The exact mechanism of screech elimination in configuration 22 is not known, but the following are possible explanations: (1) Aerodynamic changes in the flow around the flameholder were such that fluctuations in flow could not cause the cyclic vortex formation which may be part of the driving mechanism of the screech cycle; or (2) the perforated material in the flameholder itself had enough damping potential to prevent the oscillations that cause or sustain screech; or (3) the heat-release rate per unit volume near the flameholder may be a critical parameter in developing screech. Perforated gutters, like can-type flameholders and very narrow gutters, may have a more gradual heat-release zone following the initial ignition (or recirculation) region.

It is apparent, then, that for afterburner configurations having a very strong tendency to screech, perforating the flameholder will probably not solve the screech problem, since two different perforation patterns had only slight effect on screech characteristics of the 3-inch-wide single-ring flameholder. For configurations with slight or moderate screech tendencies, however, perforating the flameholder may completely eliminate screech, as was evidenced by the screech-free performance of the 2-ring, $1\frac{1}{2}$-inch-wide perforated flameholder.

Narrow-Gutter Flameholders

Although screech was noticeably more severe with the 3-inch-wide-gutter flameholder (configuration 19) than with the two $1\frac{1}{2}$-inch-wide gutters of the same blockage (configuration 4), further reduction of gutter width (for the same blockage) to four 3/4-inch-wide rings in configuration 23 did not appreciably reduce the screech tendencies of the afterburner (fig. 7(c)). Reducing the blockage from 25 to 15 percent by removing two of the four 3/4-inch-wide gutters (configuration 24) did not eliminate screech.

3943

Screened Flameholder

The purpose of the annular screen attached to flameholder E (fig. 4(g)) in configuration 25 was to damp out any longitudinal oscillations near the wall that might possibly be triggering the transverse oscillations. This configuration did not screech in the lean region of afterburner fuel-air ratios but screeched in the rich region as shown in figure 7(c).

Effect of Pressure on Screech

Previous data at afterburner-inlet pressures between 700 and 4200 pounds per square foot absolute indicate that screech would probably continue to become more severe and occur over a wider range of fuel-air ratios as burner pressure level is increased (refs. 3, 5, 6, and 14). During the present investigation, however, the following tendencies of screech with pressure were noted: (1) For configurations with medium to severe screech intensity, pressure level in the range of 4000 to 6400 pounds per square foot absolute had little if any effect on screech fuel-air-ratio limits or apparent intensity. (2) For configurations with mild screech, raising the pressure level reduced the screech intensity and also the range of fuel-air ratios in which screech occurred. This effect is illustrated in figure 12(a), which shows the boundaries of screech as a function of afterburner fuel-air ratio and pressure for configuration 3 (short fuel bars with no liner). In one case (configuration 8, long fuel bars and corrugated liner from 5 to 20 in. downstream of flameholder), screech disappeared entirely at high pressures, as shown in figure 12(b). This configuration did not screech above an afterburner-inlet pressure of about 5400 pounds per square foot absolute. These trends, which are opposite to those previously reported for lower pressure levels, are difficult to explain. It may be that, as fuel flow increased with pressure level, a slightly different fuel distribution or vaporization pattern may have existed at the flameholder that could alter the screech potential of the burner (ref. 15); or perhaps the

increase in mixture density at higher pressure levels altered the fundamental combustion kinetics in such a way as to change the time lag occurring between state changes and fluctuations of the combustion process, thus diminishing the screech driving potential as discussed in reference 12.

Differential-Pressure-Orifice Data

A typical deflection pattern of the U-tubes connected to the differential-pressure orifices of figure 6 is shown in figure 13. Even though the screech frequency that induced this pattern indicated an oscillation of the first transverse mode (ref. 5), no definite plane of oscillation is evident from the figure. This indicates that the plane of oscillation was either varying in a random fashion or had a spinning motion similar to that discussed in references 2 and 12. Either possibility is to be expected, since the afterburner geometry was circumferentially symmetrical and had nothing that would tend to stabilize the plane of oscillation. The distance from the flameholder to the region of maximum pressure fluctuation varied slightly for different configurations but was in general from 10 to 16 inches. This is in agreement with the trend of similar data given in reference 5.

SUMMARY OF RESULTS

Screech characteristics of a full-scale afterburner were investigated and several methods of screech control were evaluated over a range of afterburner-inlet pressures of from 4000 to 6400 pounds per square foot absolute. The following results were obtained:

1. A corrugated louvered liner 20 inches long completely suppressed screech at all conditions investigated, even with a 3-inch-wide flameholder gutter that had very strong screech tendencies. A 20-inch length of noncorrugated liner perforated with 3/16-inch holes on 1/2-inch centers did not entirely eliminate screech, but a 36-inch length did.

2. A 7-inch length of perforated shroud spaced radially 1/2 inch from the outer V-gutter of a 2-ring flameholder prevented screech under all conditions investigated. A similar shroud when attached directly to the gutter did not stop screech. A solid shroud 4 inches long spaced radially 1/2 inch from the outer gutter prevented screech in the rich region of operation but not in the lean region.

3. A 2-ring, $1\frac{1}{2}$-inch-wide V-gutter flameholder made from perforated metal eliminated screech over the operable range of fuel-air ratios, but a single V-gutter 3 inches wide made of the same material did not.

4. Changes in flameholder geometry that suppressed the tendency of a flameholder to shed large alternating vortices in a low-velocity flow-visualization study also moderated or eliminated the screech characteristics of the flameholder during afterburning.

5. The range of fuel-air ratios over which screech occurred and the intensity of screech remained essentially the same for most configurations as afterburner pressure was raised from approximately 4000 to 6400 pounds per square foot absolute. However, for several configurations that had only a slight tendency to screech, the range of fuel-air ratios for which screech occurred grew smaller and the screech diminished in intensity or even disappeared as pressure level was increased. This result is contrary to screech behavior previously reported at lower pressure levels.

Lewis Flight Propulsion Laboratory
National Advisory Committee for Aeronautics
Cleveland, Ohio, December 2, 1955

REFERENCES

1. Bragdon, Thomas A., Lewis, George D., and King, Charles H.: Interim Report on Experimental Investigation of High Frequency Oscillations in Ramjet Combustion Chambers. M.I.T. Meteor Rep. UAC-53, Res. Dept., United Aircraft Corp., Oct. 1951. (BuOrd Contract NOrd 9845.)

2. Smith, R. P., and Sprenger, D. F.: Combustion Instability in Solid-Propellant Rockets. Fourth Symposium (International) on Combustion, The Williams & Wilkins Co., Inc., 1953, pp. 893-906.

3. Usow, Karl H., Meyer, Carl L., and Schulze, Frederick W.: Experimental Investigation of Screeching Combustion in Full-Scale Afterburner. NACA RM E53I01, 1953.

4. Blackshear, Perry L., Rayle, Warren D., and Tower, Leonard K.: Study of Screeching Combustion in a 6-Inch Simulated Afterburner. NACA TN 3567, 1955.

5. Harp, James L., Jr., Velie, Wallace W., and Bryant, Lively: Investigation of Combustion Screech and a Method of Its Control. NACA RM E53L24b, 1954.

6. Lewis Laboratory Staff: A Summary of Preliminary Investigations into the Characteristics of Combustion Screech in Ducted Burners. NACA RM E54B02, 1954.

7. Newton, R. T., and Truman, J. C.: An Approach to the Problem of Screech in Ducted Burners. General Eng. Lab., General Electric Co., Schenectady (N.Y.), Mar. 12, 1954.

8. Fuels and Combustion Research Division: Adaptation of Combustion Principles to Aircraft Propulsion. Vol. I - Basic Considerations in the Combustion of Hydrocarbon Fuels with Air. NACA RM E54I07, 1955.

9. Henzel, James G., Jr., and Bryant, Lively: Investigation of Effect of Number and Width of Annular Flame-Holder Gutters on Afterburner Performance. NACA RM E54C30, 1954.

10. Kaskan, W. E., and Noreen, A. E.: High-Frequency Oscillations of a Flame Held by a Bluff Body. A.S.M.E. Trans., vol. 77, no. 6, Aug. 1955, pp. 885-891; discussion, pp. 891-895.

11. Rogers, Don E., and Marble, Frank E.: A Mechanism for High Frequency Oscillation in Ramjet Combustors and Afterburners. Heat Transfer and Fluid Mech. Inst., Univ. Calif., 1955.

12. Moore, Franklin K., and Maslen, Stephen H.: Transverse Oscillations in a Cylindrical Combustion Chamber. NACA TN 3152, 1954.

13. Younger, George G., Gabriel, David S., and Mickelsen, William R.: Experimental Study of Isothermal Wake-Flow Characteristics of Various Flame-Holder Shapes. NACA RM E51K07, 1952.

14. Conrad, E. William, Schulze, Frederick W., and Usow, Karl H.: Effect of Diffuser Design, Diffuser-Exit Velocity Profile, and Fuel Distribution on Altitude Performance of Several Afterburner Configurations. NACA RM E53A30, 1953.

15. Useller, James W., and Povolny, John H.: Experimental Investigation of Turbojet-Engine Thrust Augmentation by Combined Compressor Coolant Injection and Tail-Pipe Burning. NACA RM E51H16, 1951.

TABLE I. - AFTERBURNER CONFIGURATIONS

Configuration	Flameholder		Combustor liner		Fuel-spray bars		Cooling system
	Type	Figure	Type	Figure	Type	Figure	
1	A	4(a)	L1	5(c)	Short	3(b)	Original
2	A	↓	L2	5(d)	Long	3(c)	Modified
3	A	↓	None		Short	3(b)	↓
4	A	↓	None		Long	3(c)	↓
5	D1	4(e)	L2	5(d)	↓	↓	↓
6	A	4(a)	L3	5(d)	↓	↓	↓
7	A	↓	L4	5(e)	↓	↓	↓
8	A	↓	L5	5(f)	↓	↓	↓
9	A	↓	L6	5(g)	↓	↓	↓
10	A	↓	L7	5(h)	↓	↓	↓
11	C1	4(d)	None		↓	↓	↓
12	C2	↓	↓		↓	↓	↓
13	C3	↓	↓		↓	↓	↓
14	C4	↓	↓		↓	↓	↓
15	C5	↓	↓		↓	↓	↓
16	C6	↓	↓		↓	↓	↓
17	C7	↓	↓		↓	↓	↓
18	C8	↓	↓		↓	↓	↓
19	D1	4(e)	↓		↓	↓	↓
20	D2	4(e)	↓		↓	↓	↓
21	D3	[a]4(e)	↓		↓	↓	↓
22	D4	4(f)	↓		↓	↓	↓
23	B1	4(b)	↓		↓	↓	↓
24	B2	4(c)	↓		↓	↓	↓
25	E	4(g)	↓		↓	↓	↓

[a]Perforated with 3/16" holes on 1/2" centers.

[redacted]

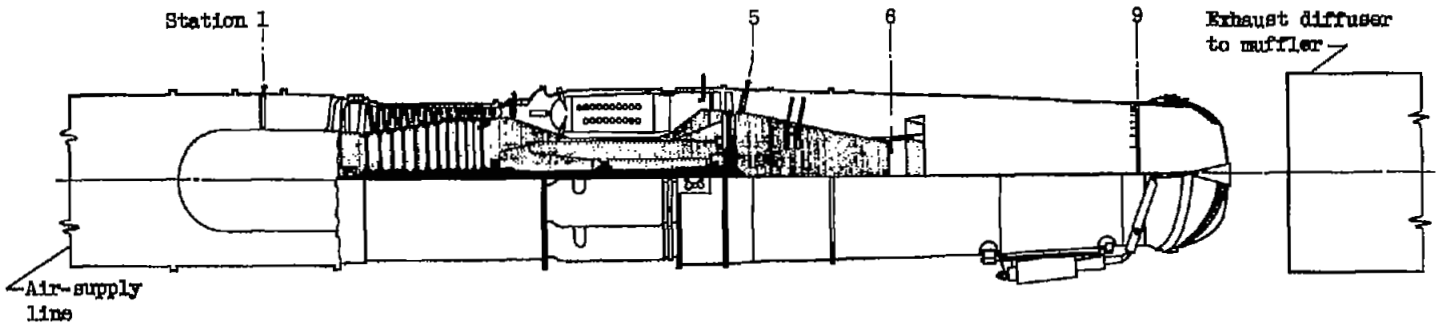

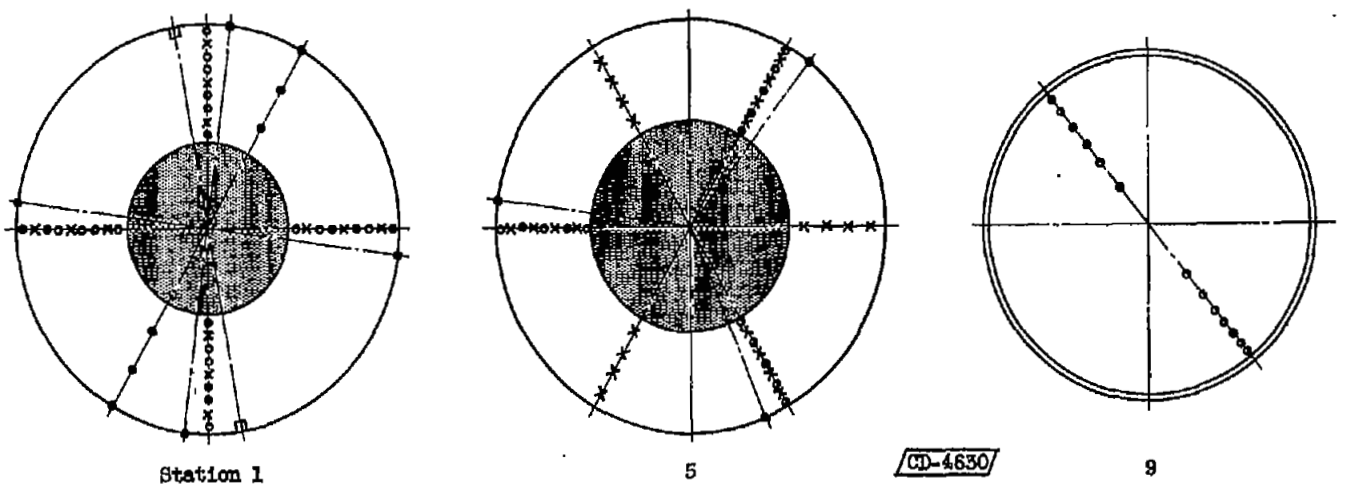

o Total pressure

• Static pressure

× Temperature

□ Boundary-layer survey

Figure 1. - Schematic view of engine and afterburner showing instrumentation stations.

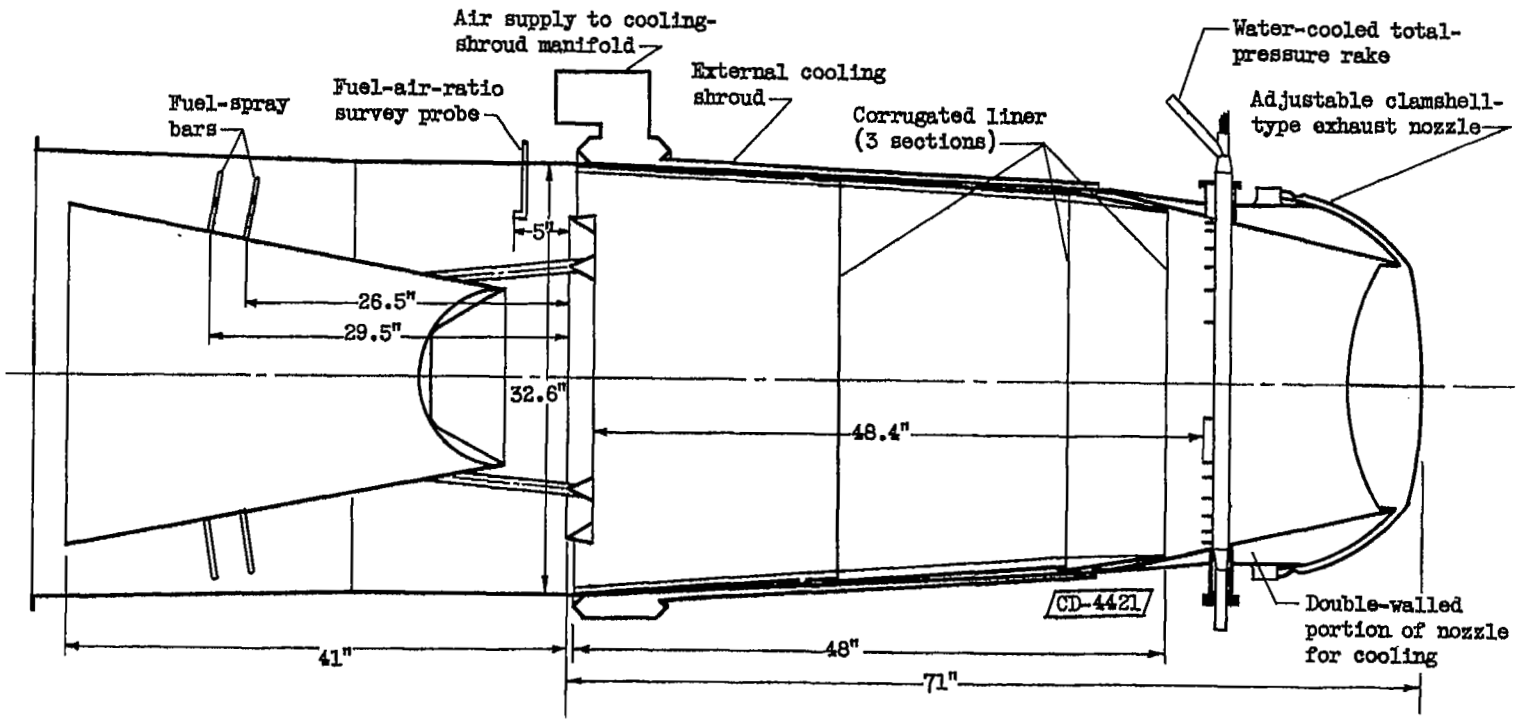

Figure 2. - Afterburner with 48-inch liner and cooling shroud.

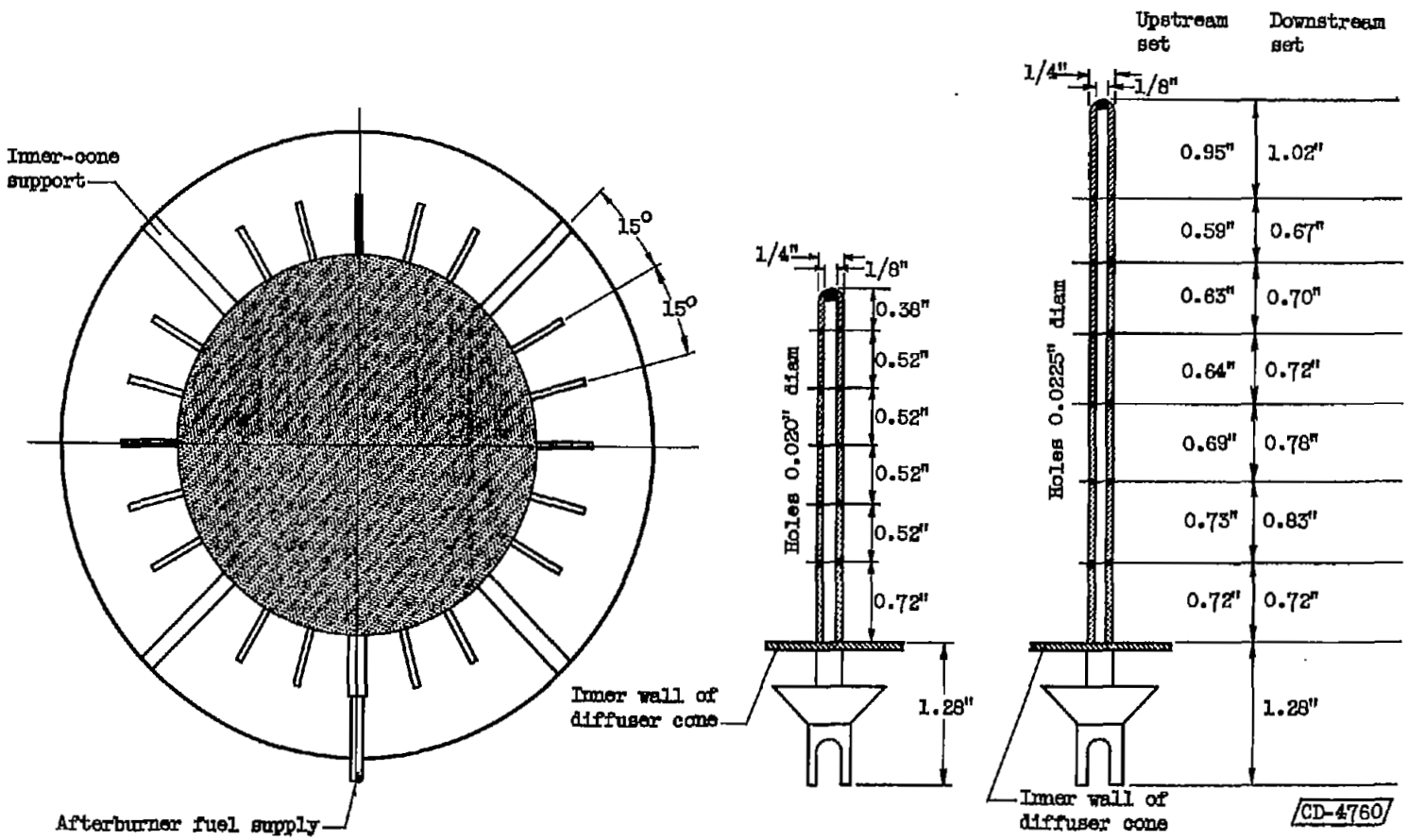

(a) Circumferential location of spray bars. (b) "Short" set. (c) "Long" set.

Figure 3. - Fuel-spray-bar configurations.

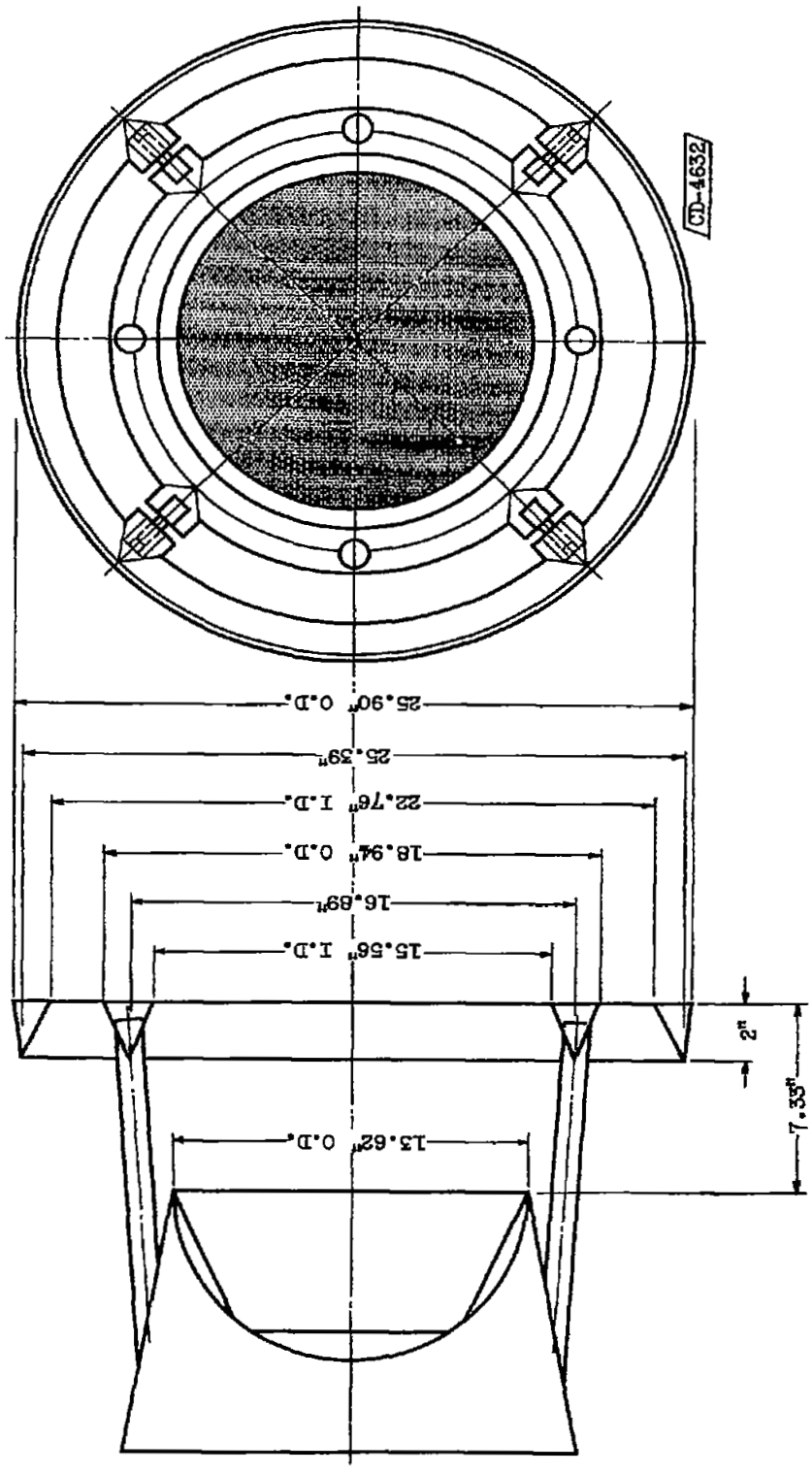

(a) Type A (27-percent blockage): 2-ring, $1\frac{1}{2}$-inch-wide V-gutter flameholder.

Figure 4. - Flameholders investigated.

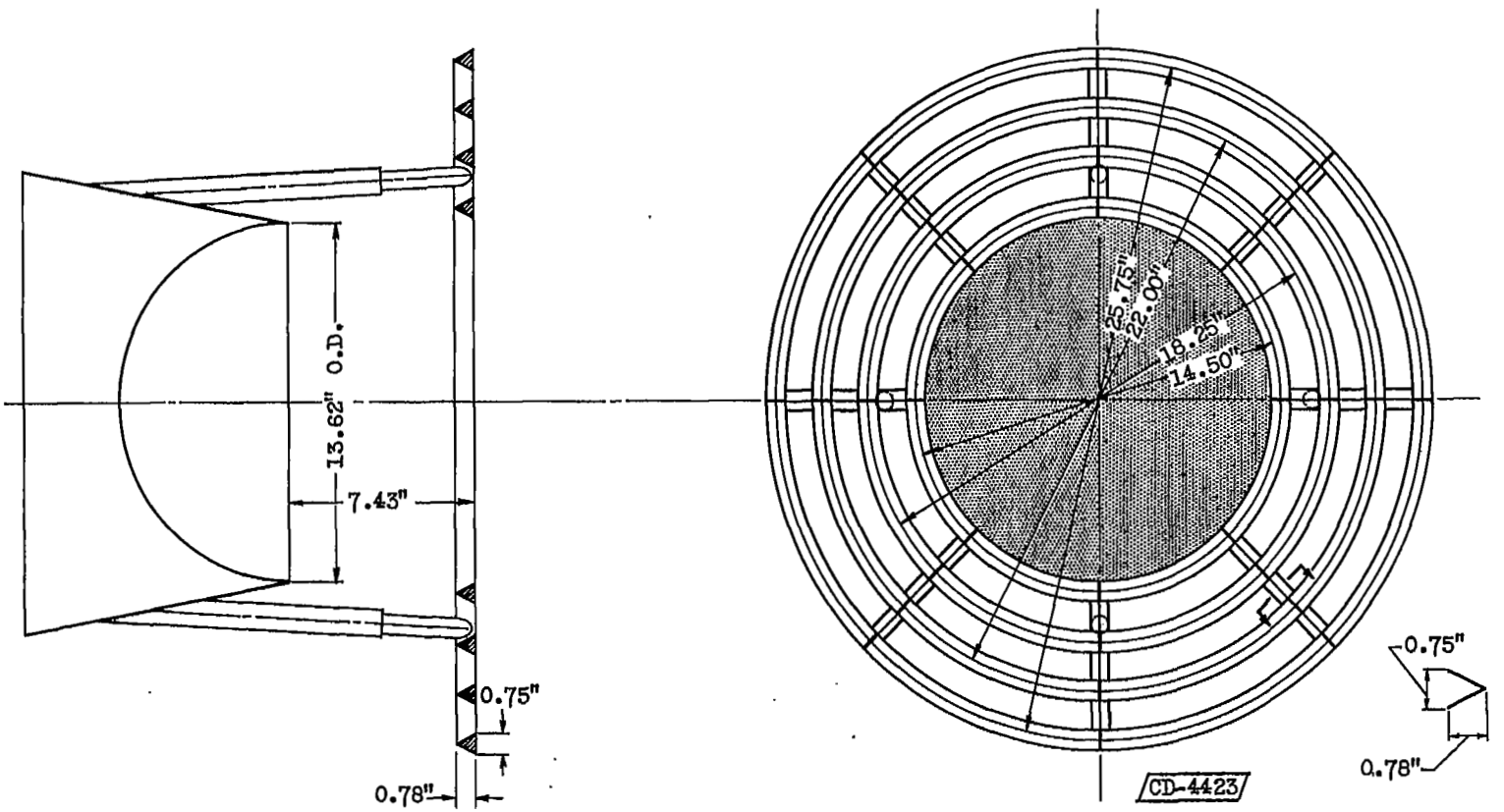

(b) Type B1 (25-percent blockage): 4-ring, 3/4-inch-wide V-gutter flameholder.

Figure 4. - Continued. Flameholders investigated.

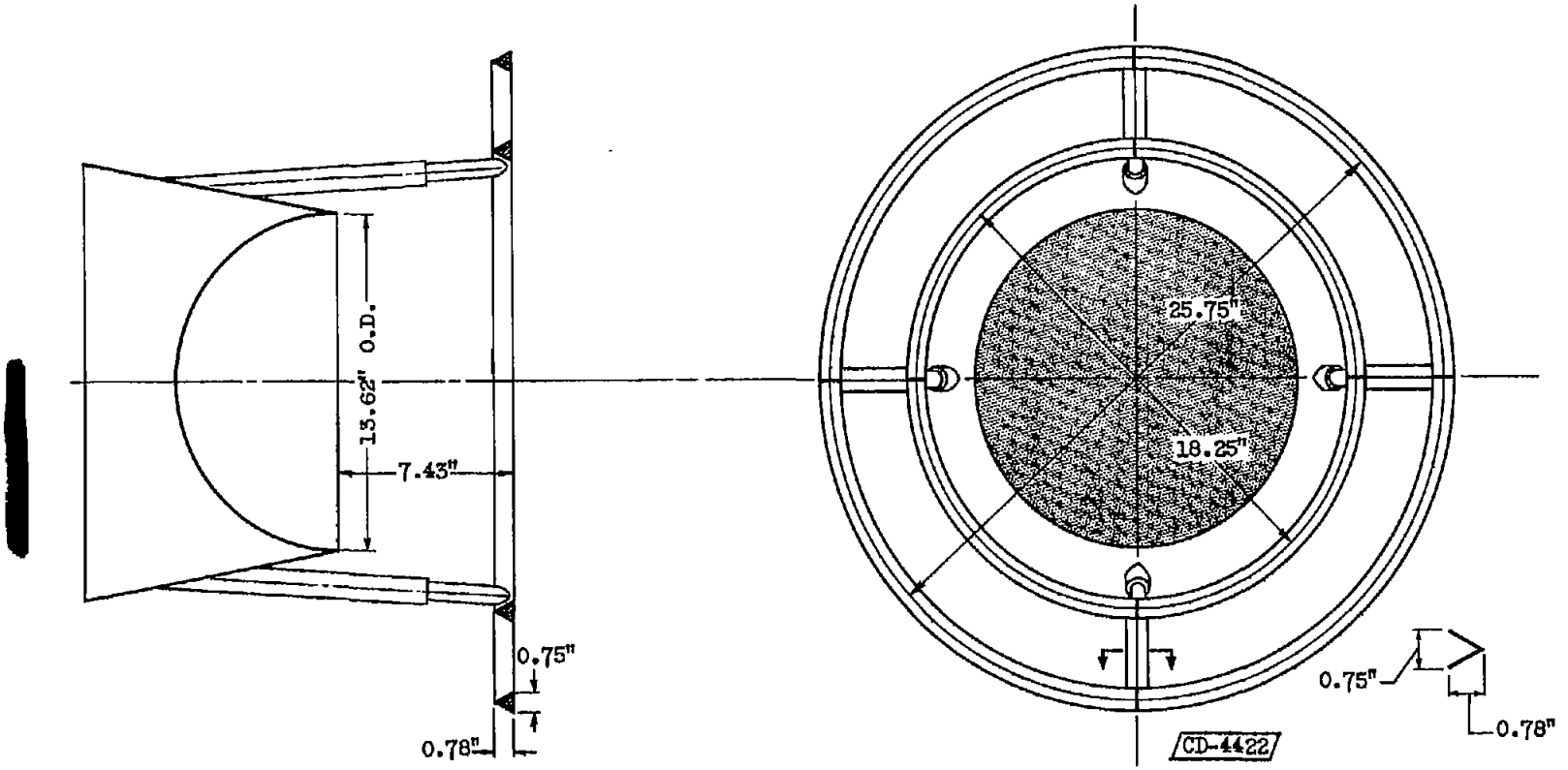

(c) Type B2 (15-percent blockage): 2-ring, 3/4-inch-wide V-gutter flameholder.

Figure 4. - Continued. Flameholders investigated.

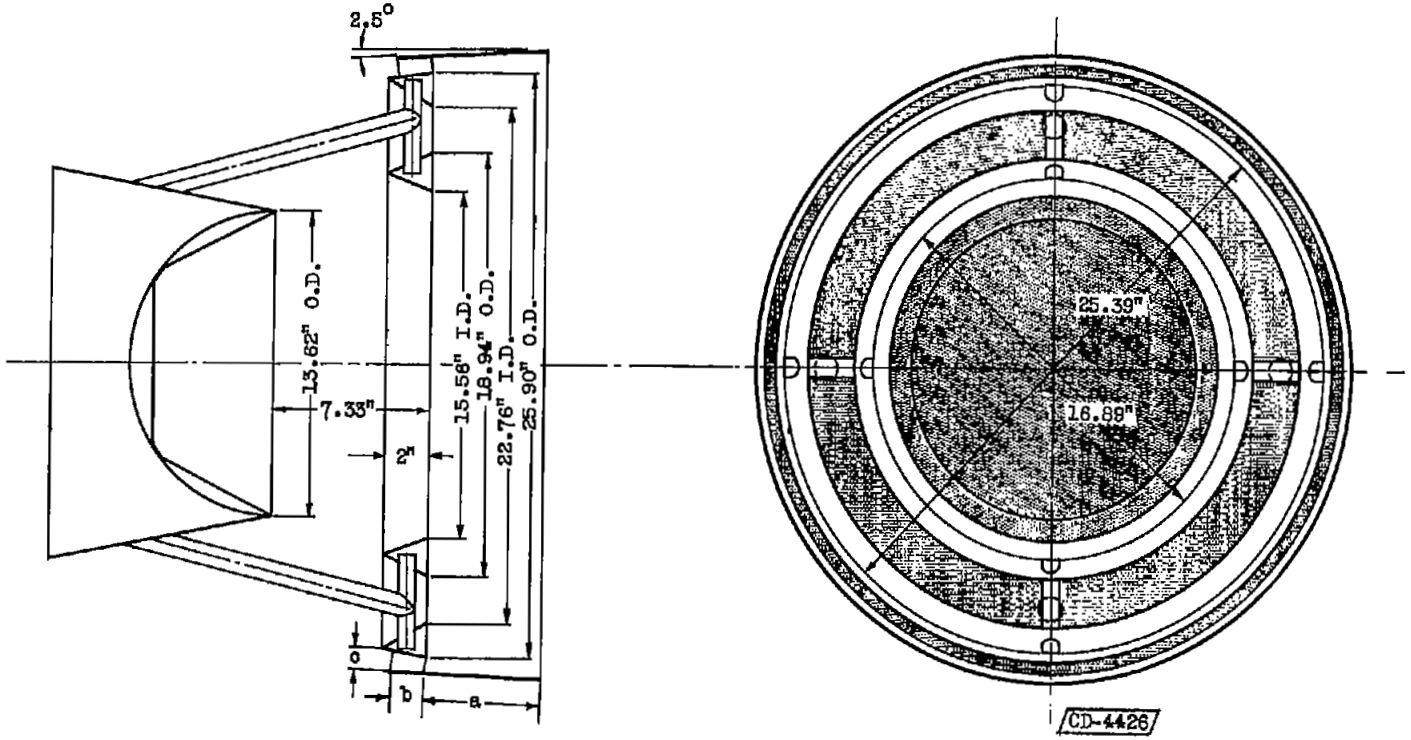

Flame-holder	Configurations	a, in.	b, in.	c, in.	Shroud perforated[1]
C1	11	8.5	1.5	0.5	Yes
C2	12	5.5	1.5		
C3	13	2.5	1.5		
C4	14	2.5	0		
C5	15	2.5	1.5		No
C6	16	5.5	1.5		
C7	17	8.5	1.5		
C8	18	5.5	0	0	Yes

[1]Holes 3/16" diam. on 1/2" centers.

(d) Type C (about 27-percent blockage): shrouded flameholders.

Figure 4. - Continued. Flameholders investigated.

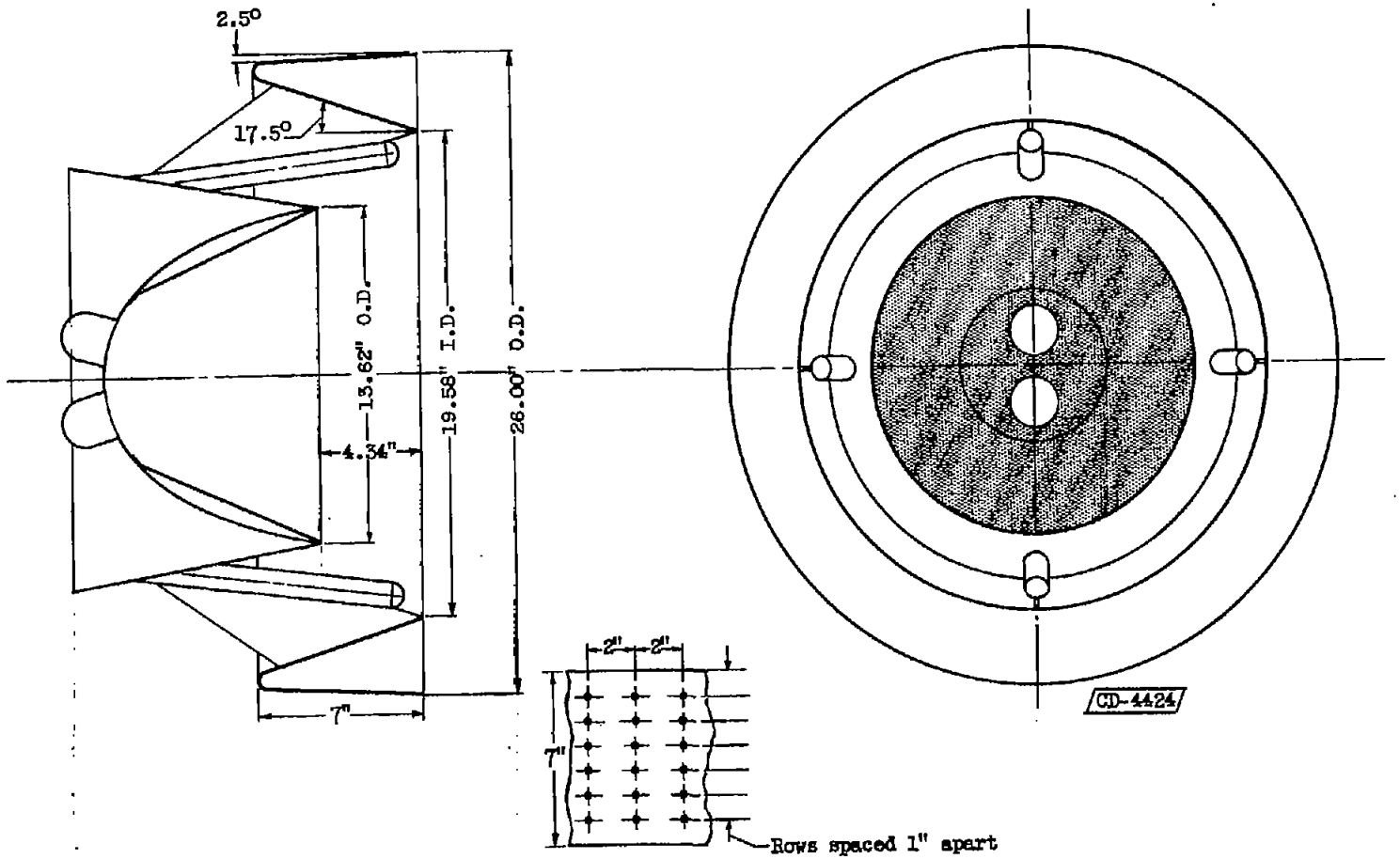

Perforation pattern for wide-gutter flameholder with 1/2" holes (type D2)

(e) Types D1 and D2 (about 27-percent blockage without perforations): single-ring wide-gutter flameholder. (Type D1 unperforated.)

Figure 4. - Continued. Flameholders investigated.

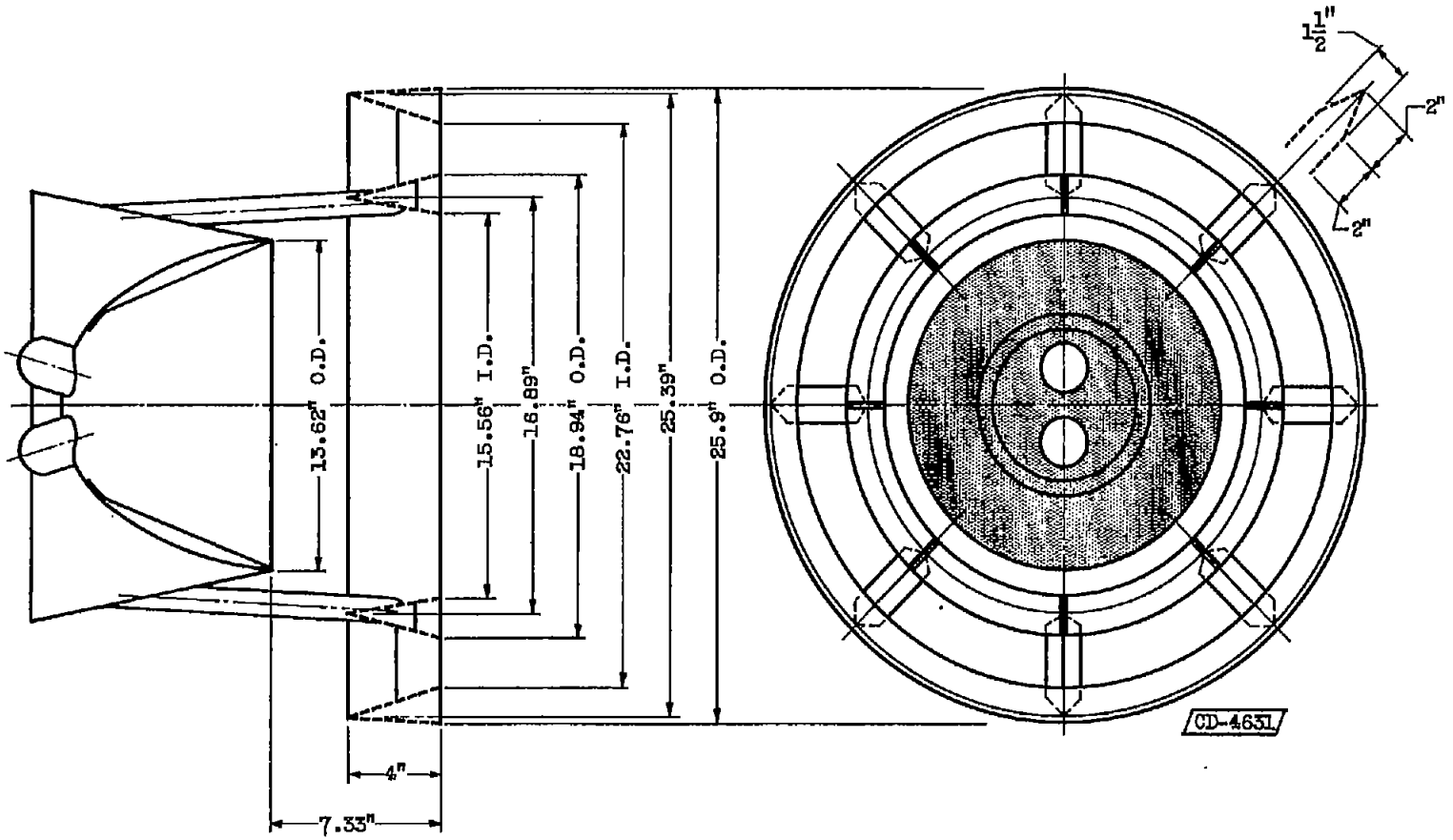

(f) Type D4 (27-percent blockage without perforations): 2 ring perforated V-gutter flameholder.

Figure 4. - Continued. Flameholders investigated.

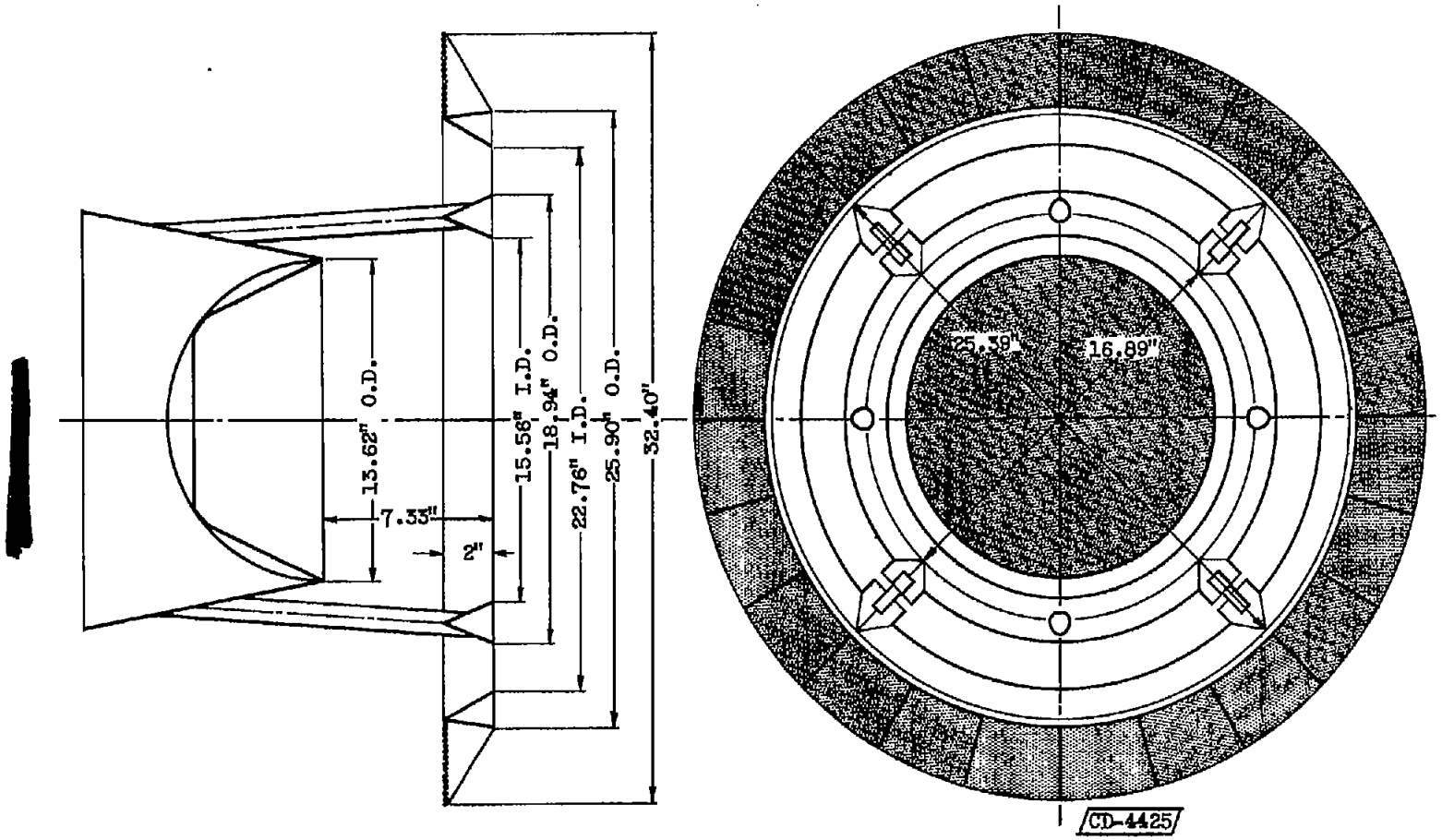

(g) Type E (48-percent blockage): 2 ring V-gutter flameholder with annular screen.

Figure 4. - Concluded. Flameholders investigated.

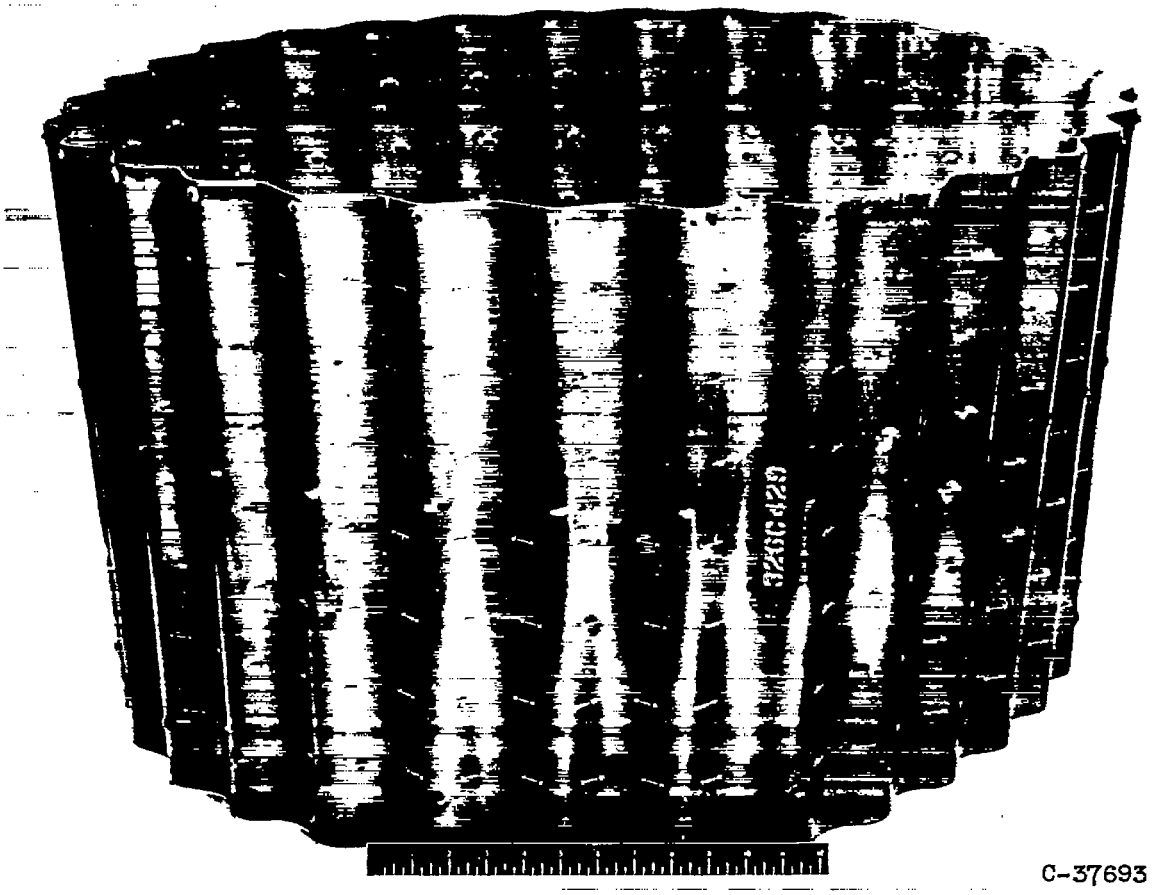

(a) Section of corrugated louvered liner.

Figure 5. - Combustion-chamber-liner configurations.

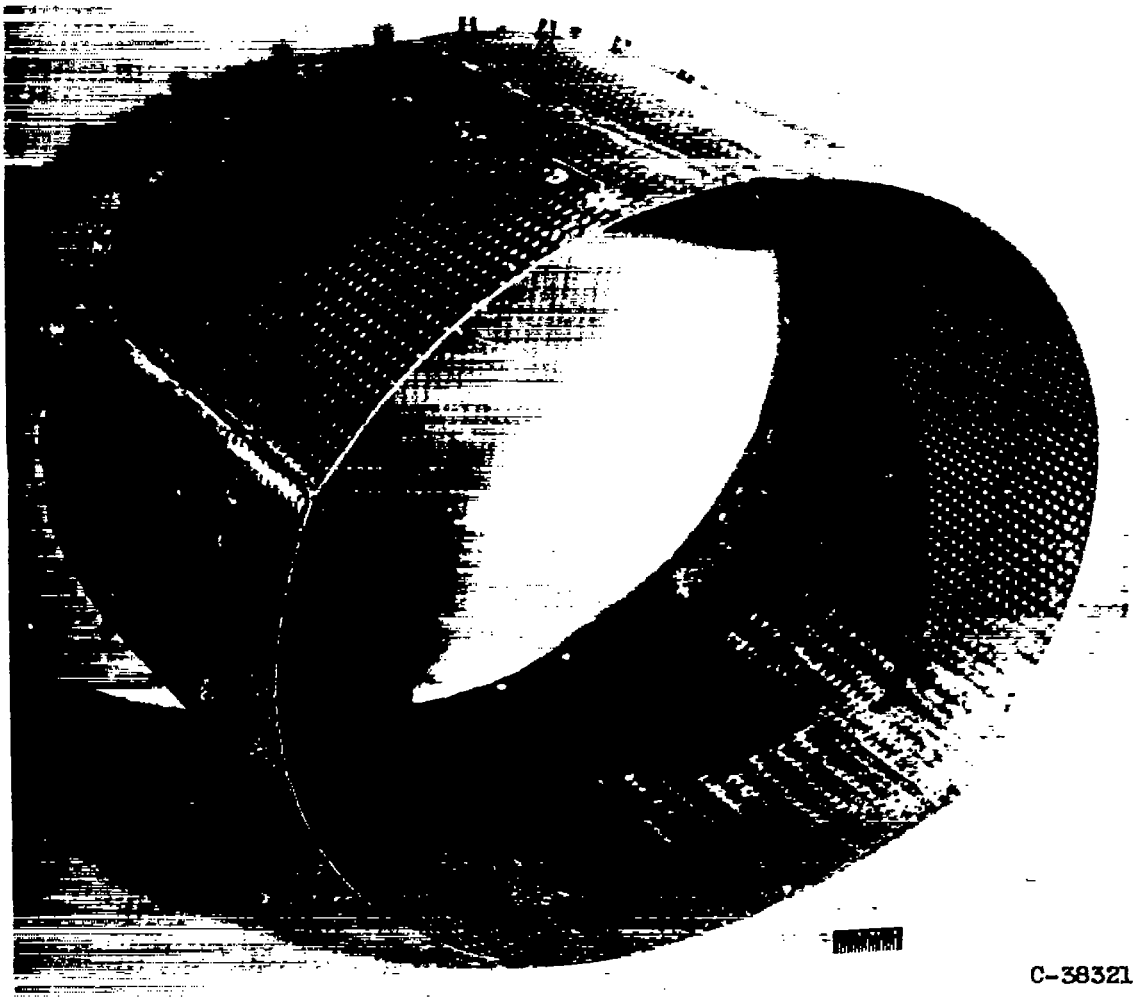

(b) Noncorrugated perforated liner.

Figure 5. - Continued. Combustion-chamber-liner configurations.

Corrugated louvered liners

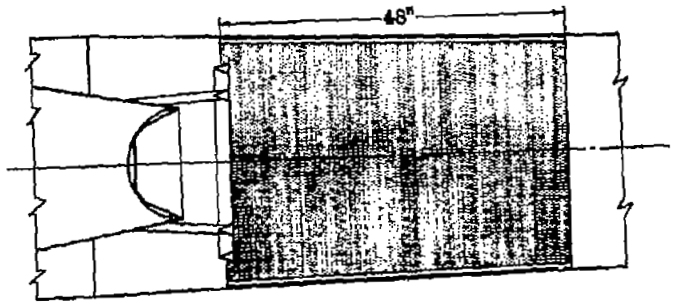

(a) Liner L1.

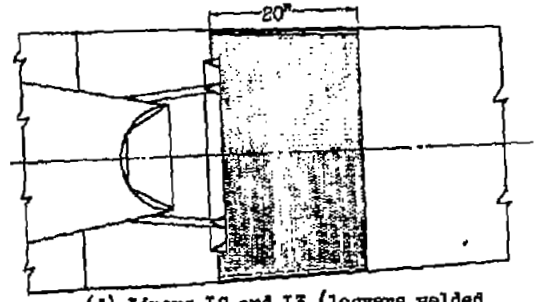

(d) Liners L2 and L3 (louvers welded shut on liner L3).

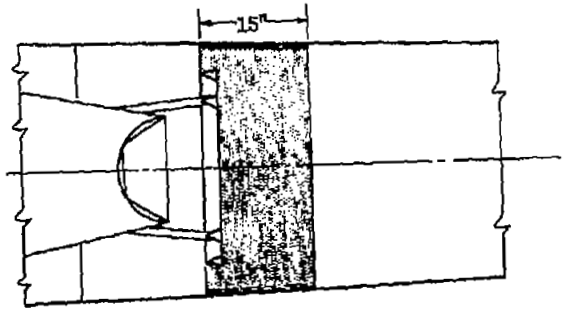

(e) Liner L4.

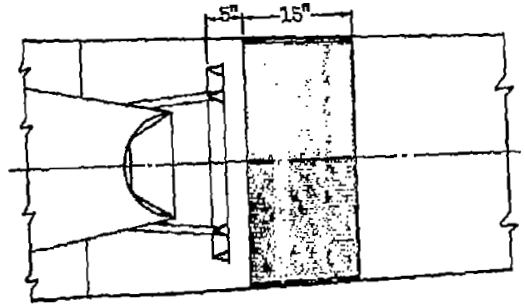

(f) Liner L5.

Nonocorrugated perforated liners

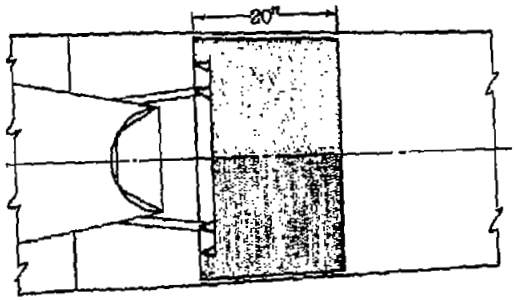

(g) Liner L6.

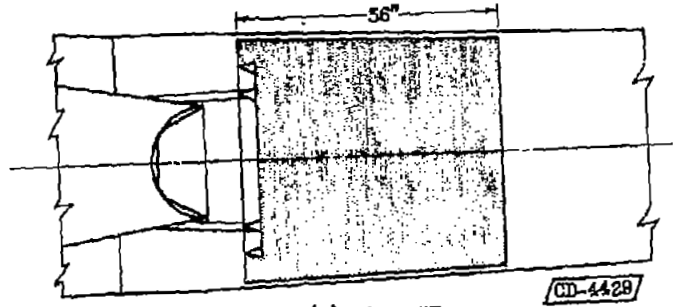

(h) Liner L7.

Figure 5. - Concluded. Combustion-chamber-liner configurations.

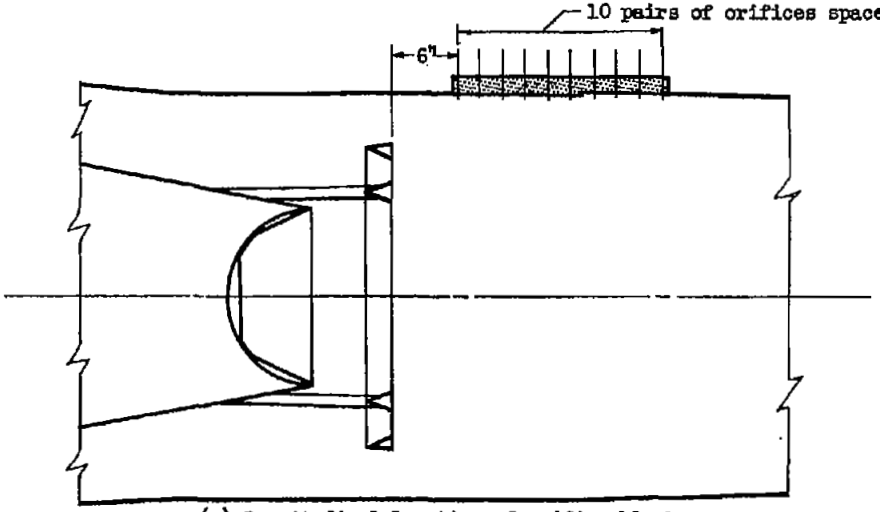

(a) Longitudinal location of orifice blocks.

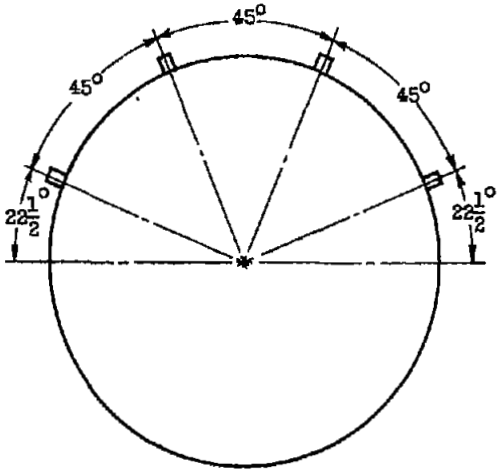

(b) Circumferential location of orifice blocks.

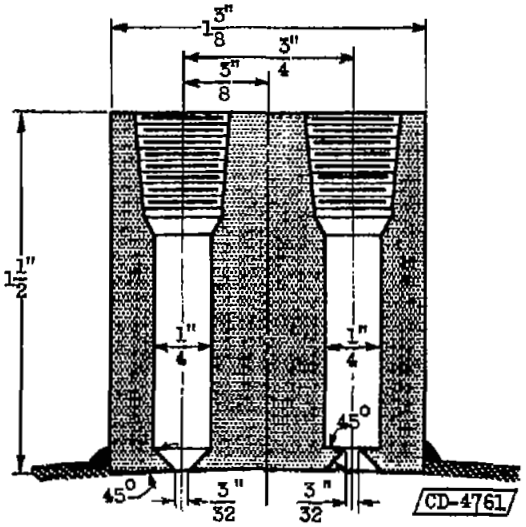

(c) Cross section of block showing one pair of differential pressure orifices.

Figure 8. - Differential pressure orifices.

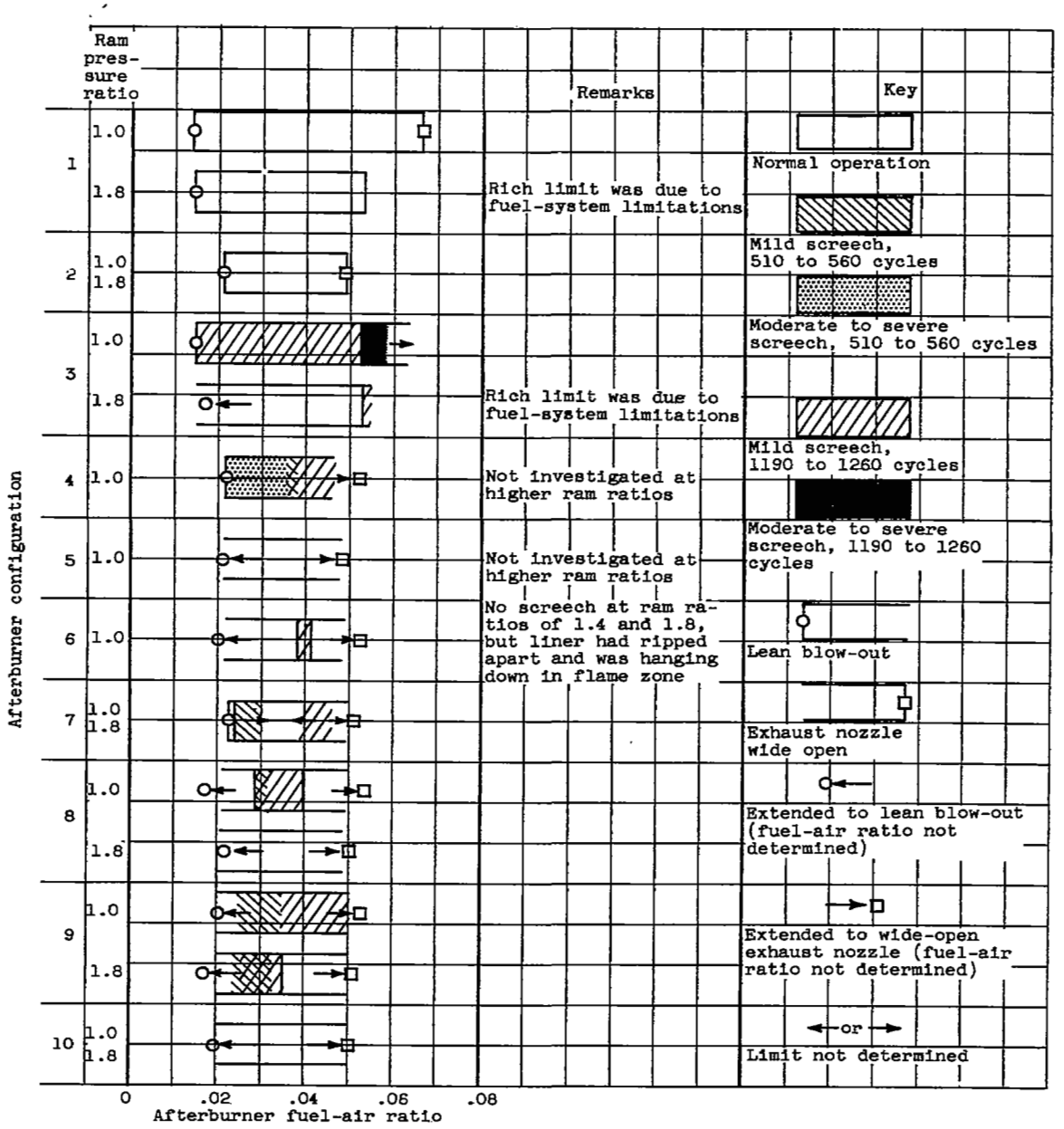

(a) Configurations 1 to 10.

Figure 7. - Operational characteristics of various afterburner configurations.

[redacted]

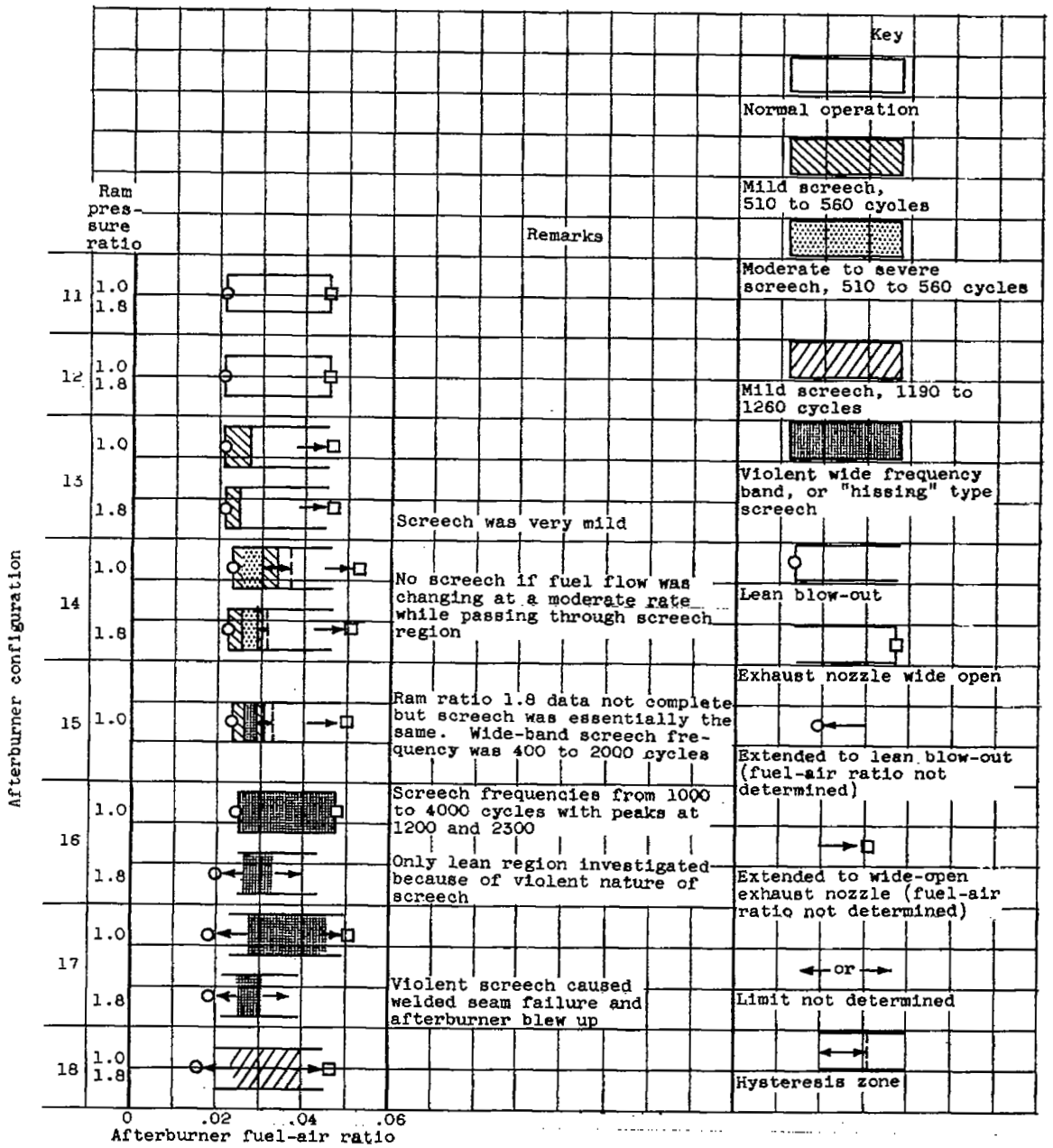

(b) Configurations 11 to 18.

Figure 7. - Continued. Operational characteristics of various afterburner configurations.

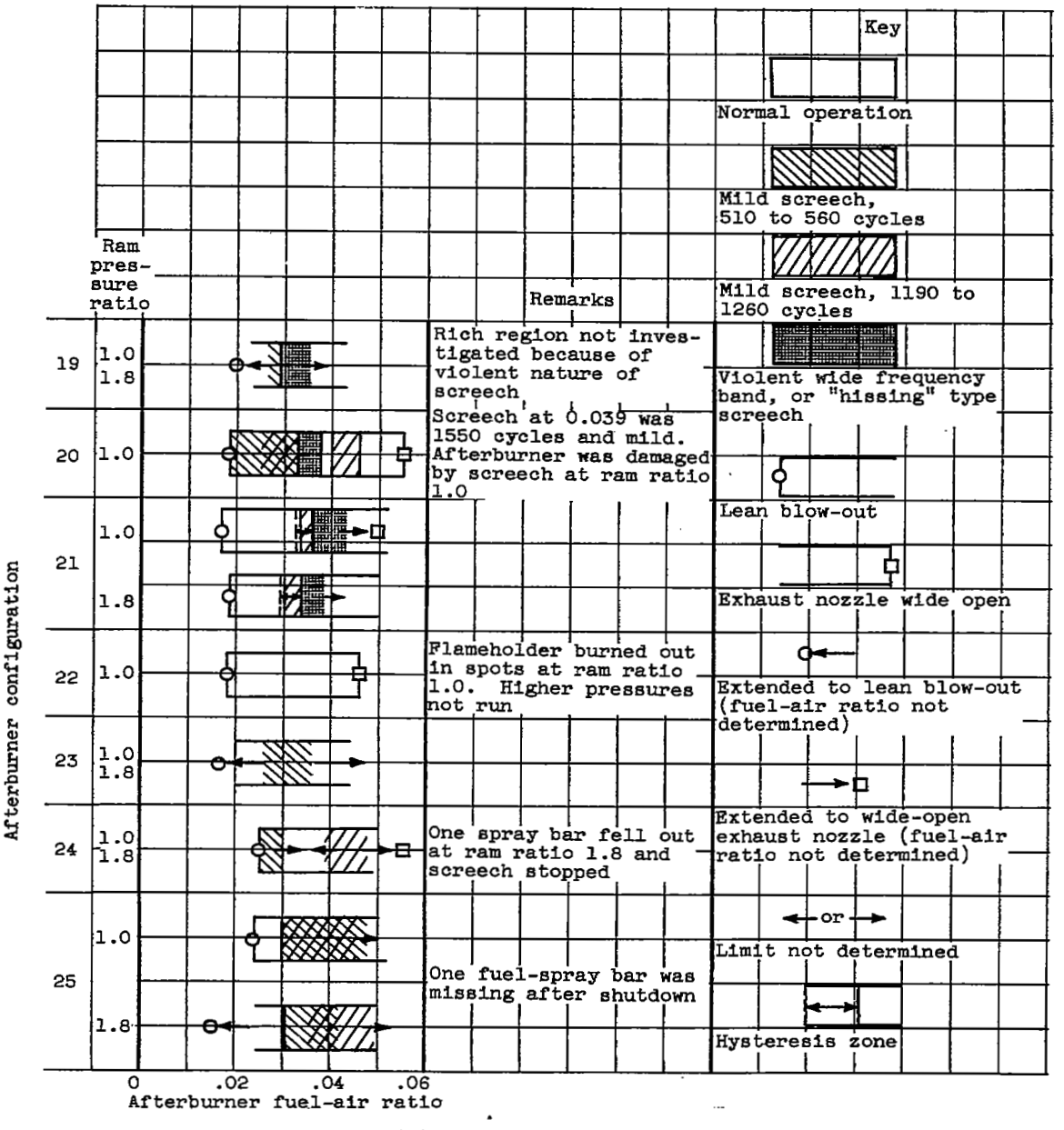

(c) Configurations 19 to 25.

Figure 7. - Concluded. Operational characteristics of various afterburner configurations.

[redacted]

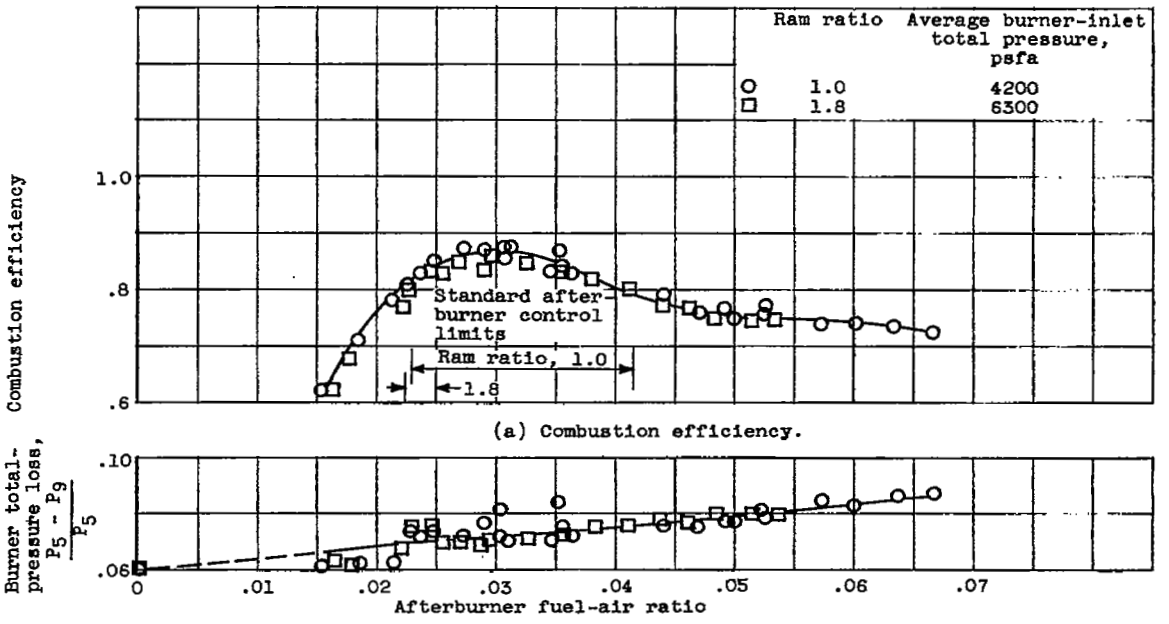

(a) Combustion efficiency.

(b) Burner total-pressure loss.

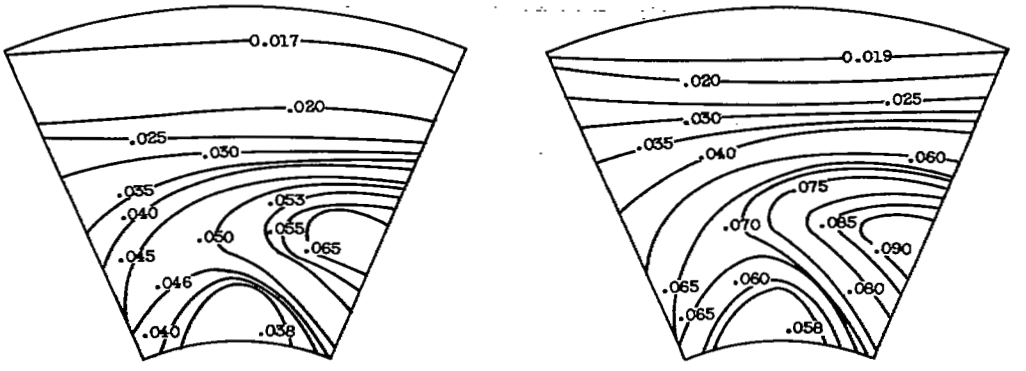

Afterburner fuel-air ratio, 0.025 Afterburner fuel-air ratio, 0.040

(c) Contours of total fuel-air ratio surveyed ahead of flameholder.

Figure 8. - Afterburner performance of configuration 1 ("short" set of fuel bars; 2-ring, $1\frac{1}{2}$-inch-wide V-gutter flameholder A; 48-inch corrugated louvered liner L1).

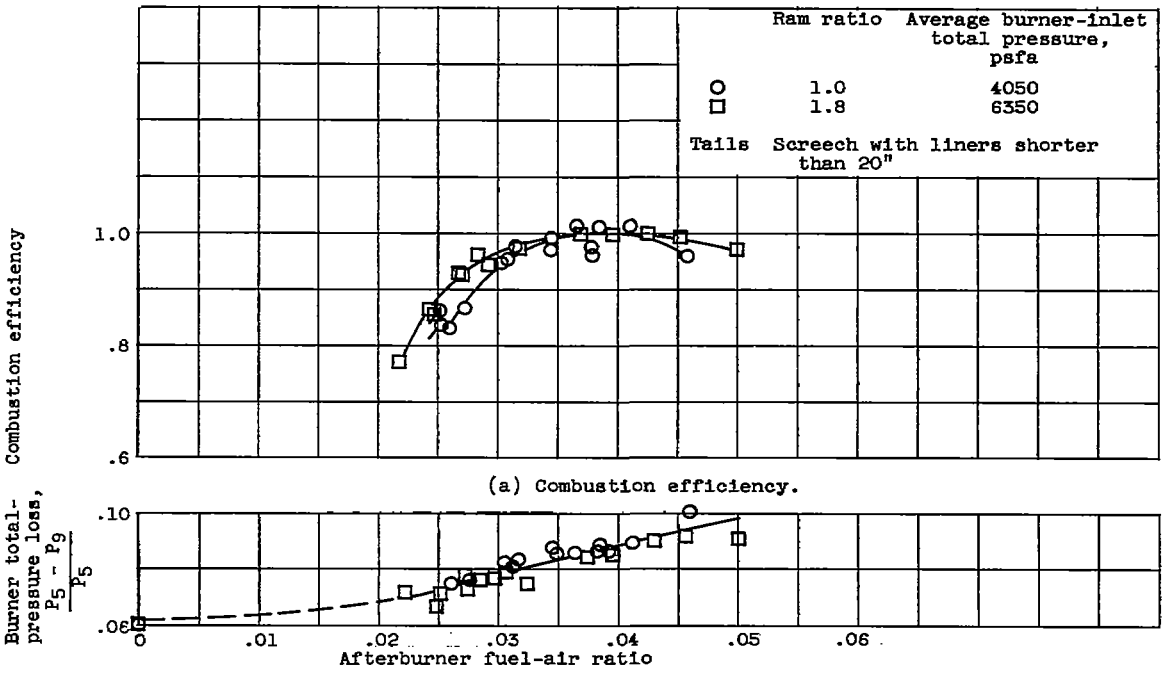

(a) Combustion efficiency.

(b) Burner total-pressure loss.

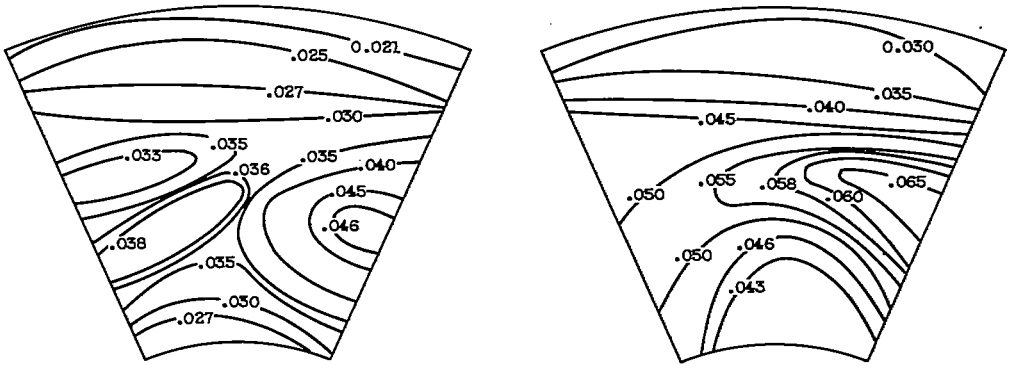

Afterburner fuel-air ratio, 0.025 Afterburner fuel-air ratio, 0.040

(c) Contours of total fuel-air ratio surveyed ahead of flameholder.

Figure 9. - Afterburner performance of configuration 2 ("long" set of fuel bars; 2-ring, $1\frac{1}{2}$-inch-wide V-gutter flameholder A; 20-inch corrugated louvered liner L2).

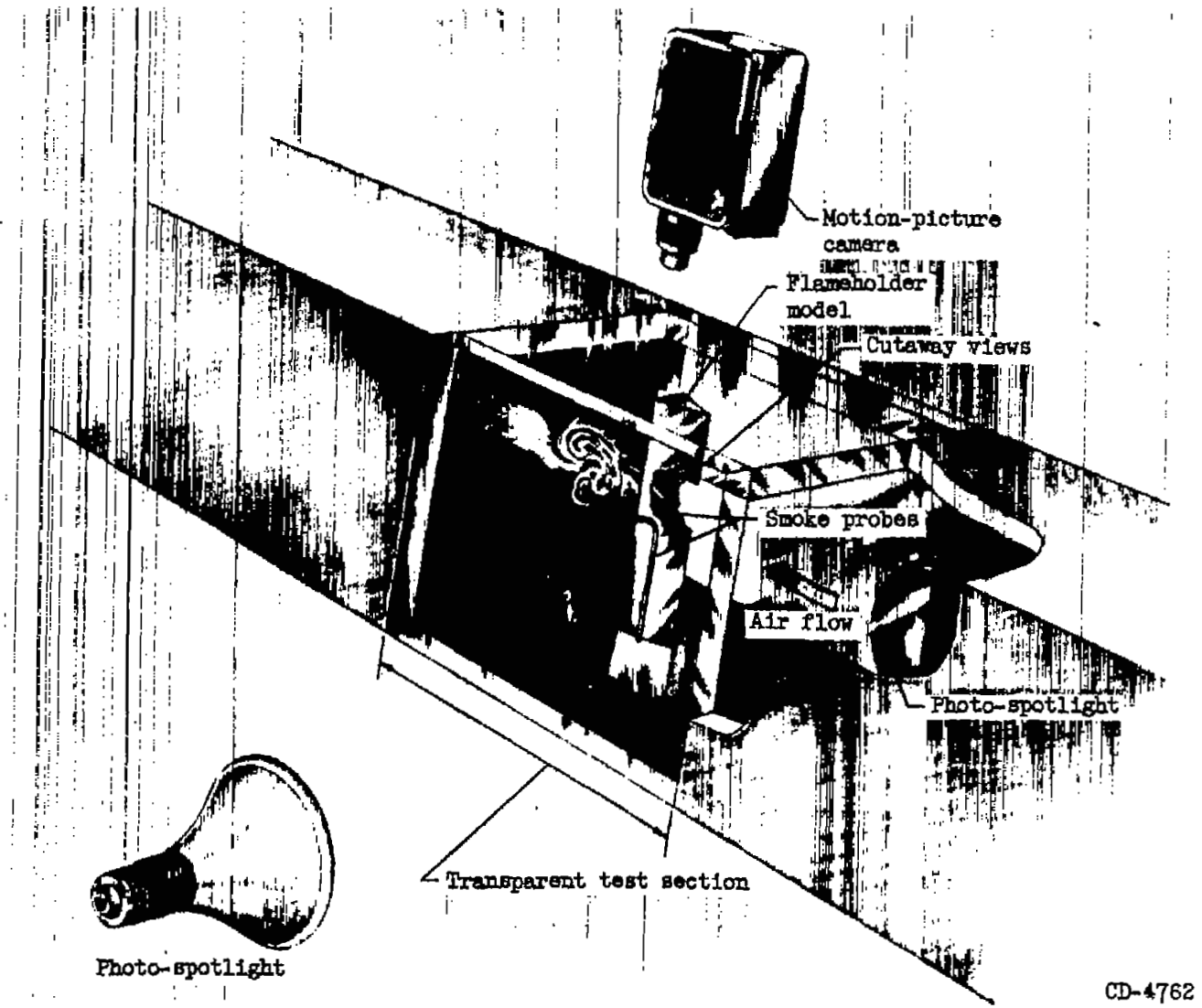

Figure 10. - Test section of low-velocity wind tunnel used in flow-visualization studies.

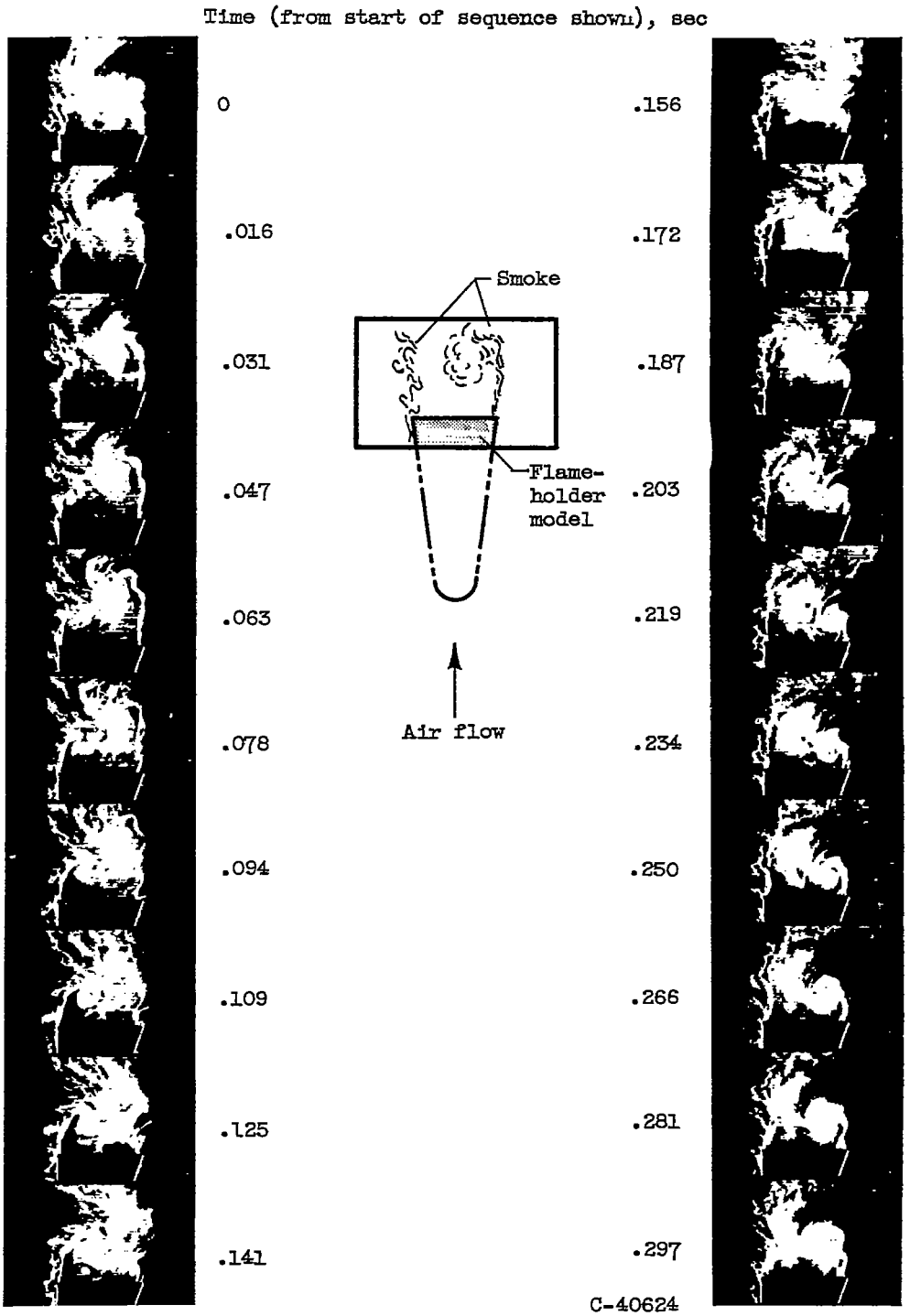

(a) Solid 3-inch-wide gutter.

Figure 11. - Smoke patterns in wake of flameholder models.

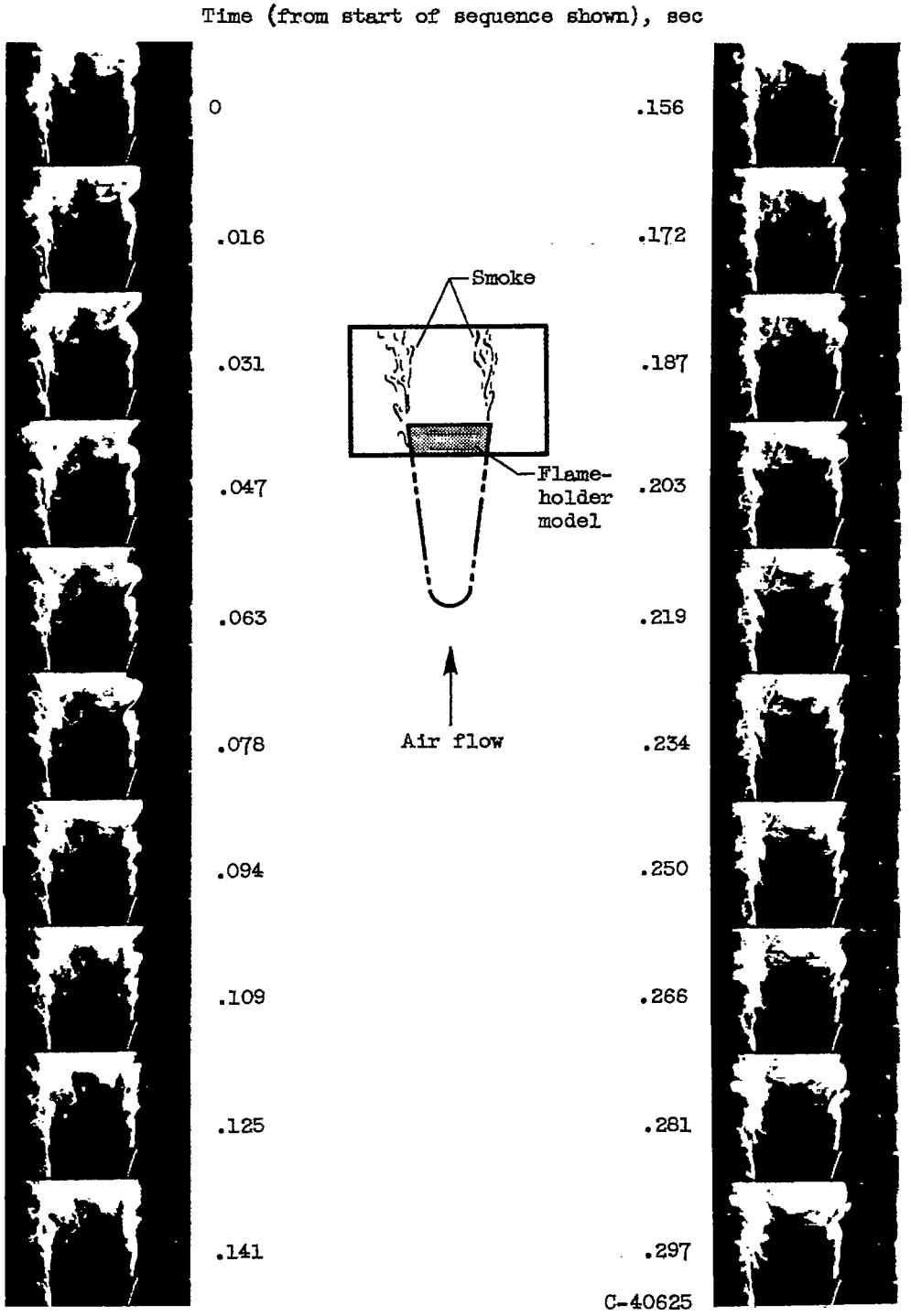

(b) Perforated 3-inch-wide gutter.

Figure 11. - Continued. Smoke patterns in wake of flameholder models.

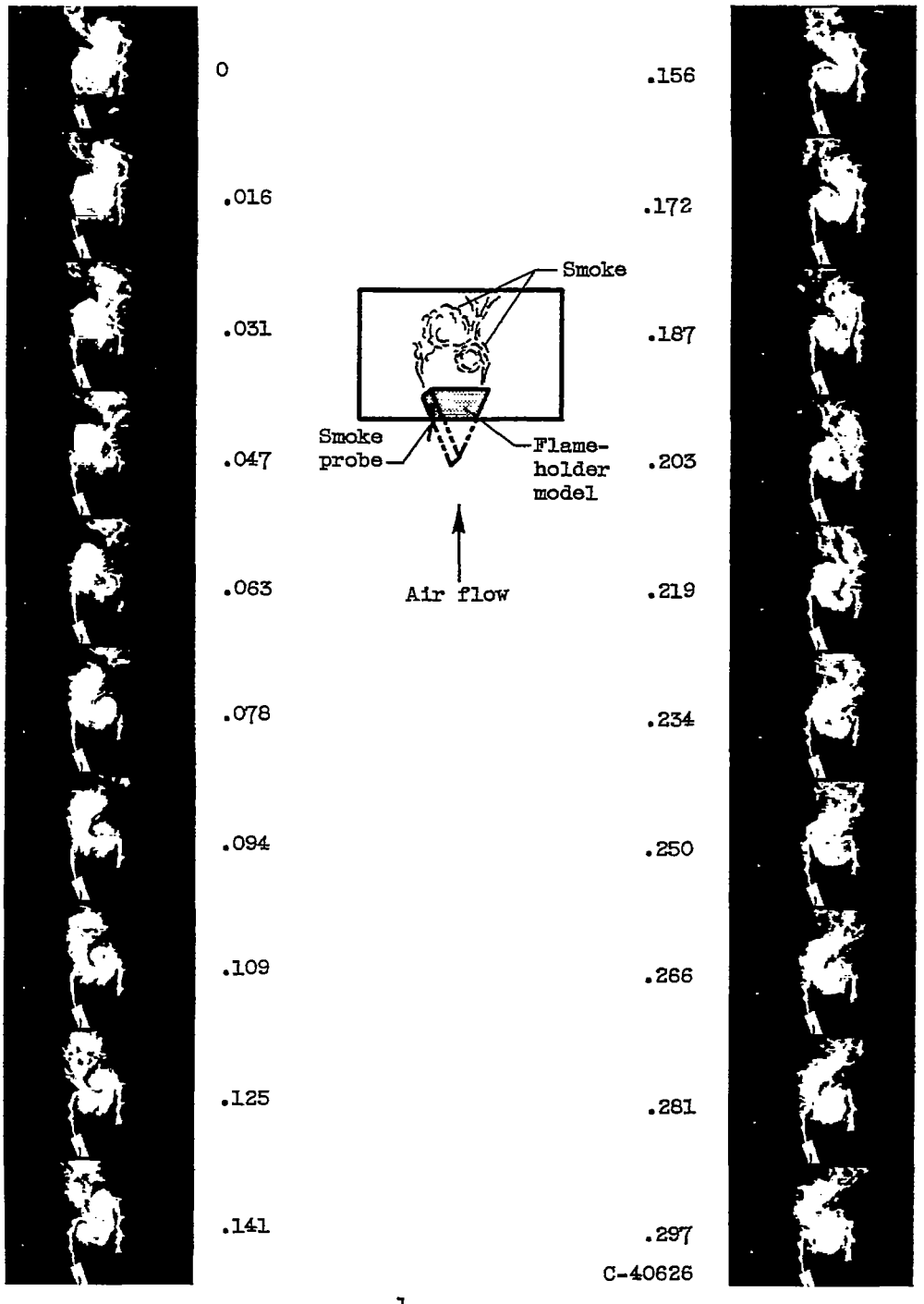

(c) Plain $1\frac{1}{2}$-inch-wide V-gutter.

Figure 11. - Continued. Smoke patterns in wake of flameholder models.

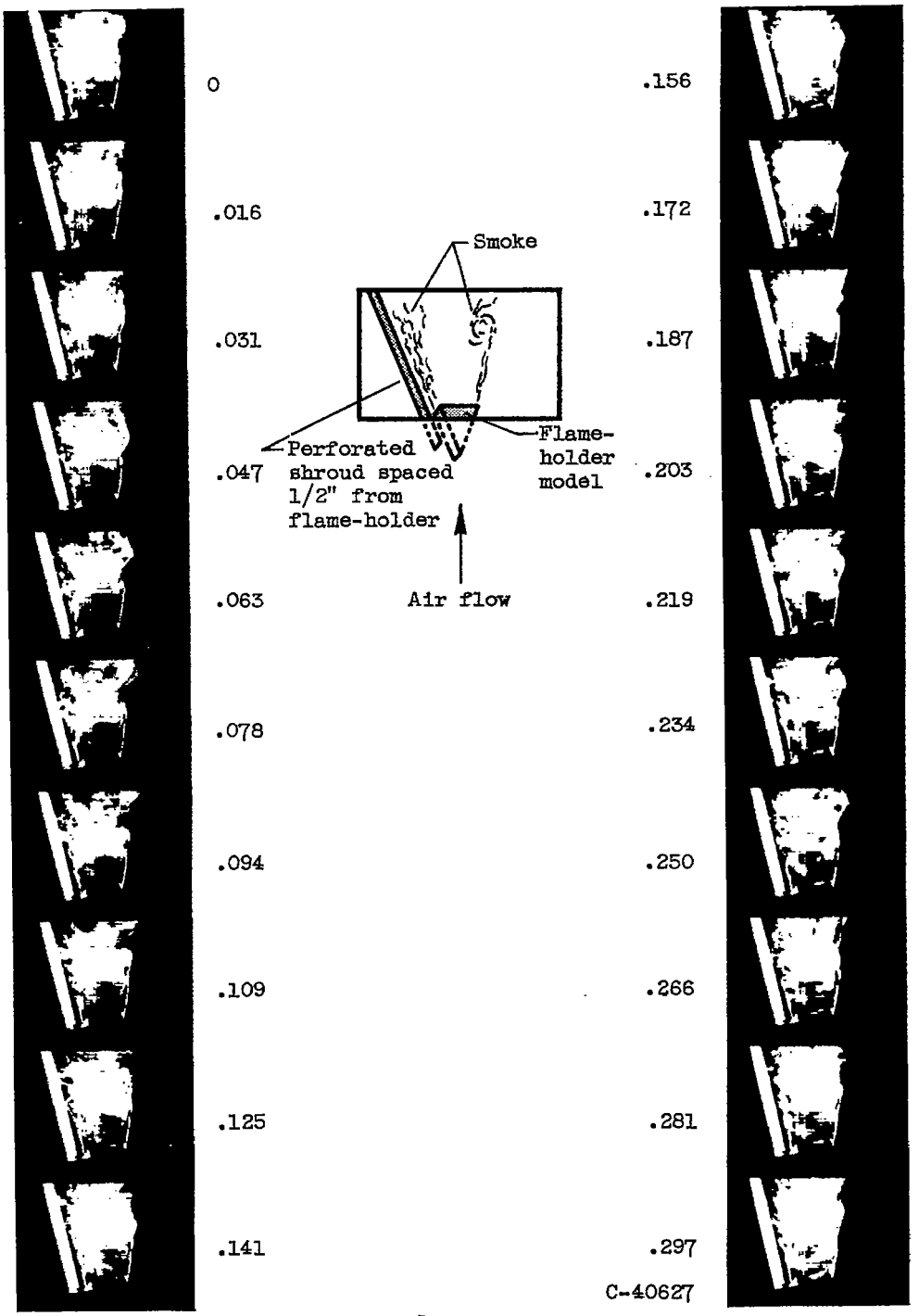

(d) Shrouded $1\frac{1}{2}$-inch-wide V-gutter.

Figure 11. - Concluded. Smoke patterns in wake of flameholder models.

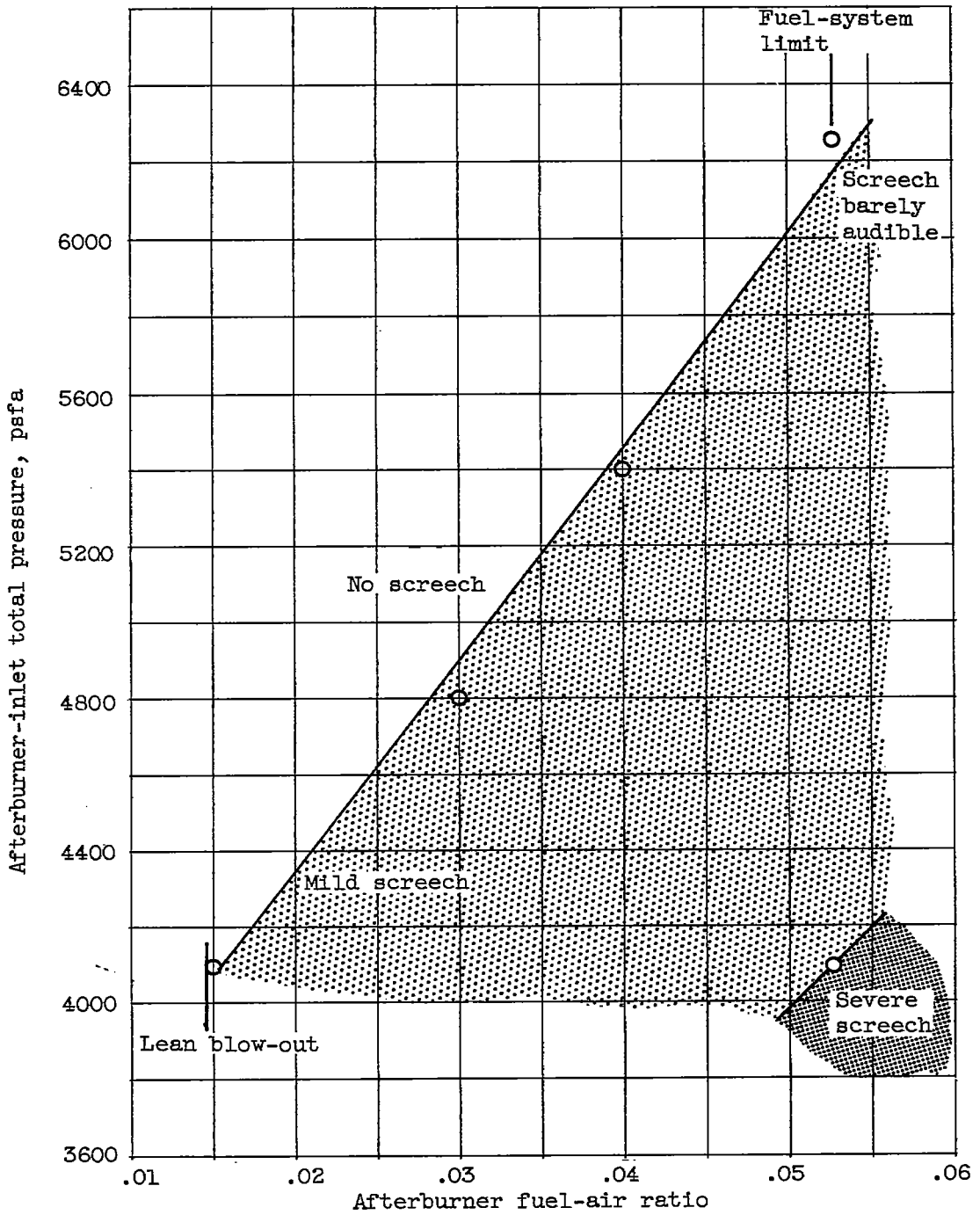

(a) Configuration 3.

Figure 12. - Effect of pressure and fuel-air ratio on screech boundaries.

[redacted]

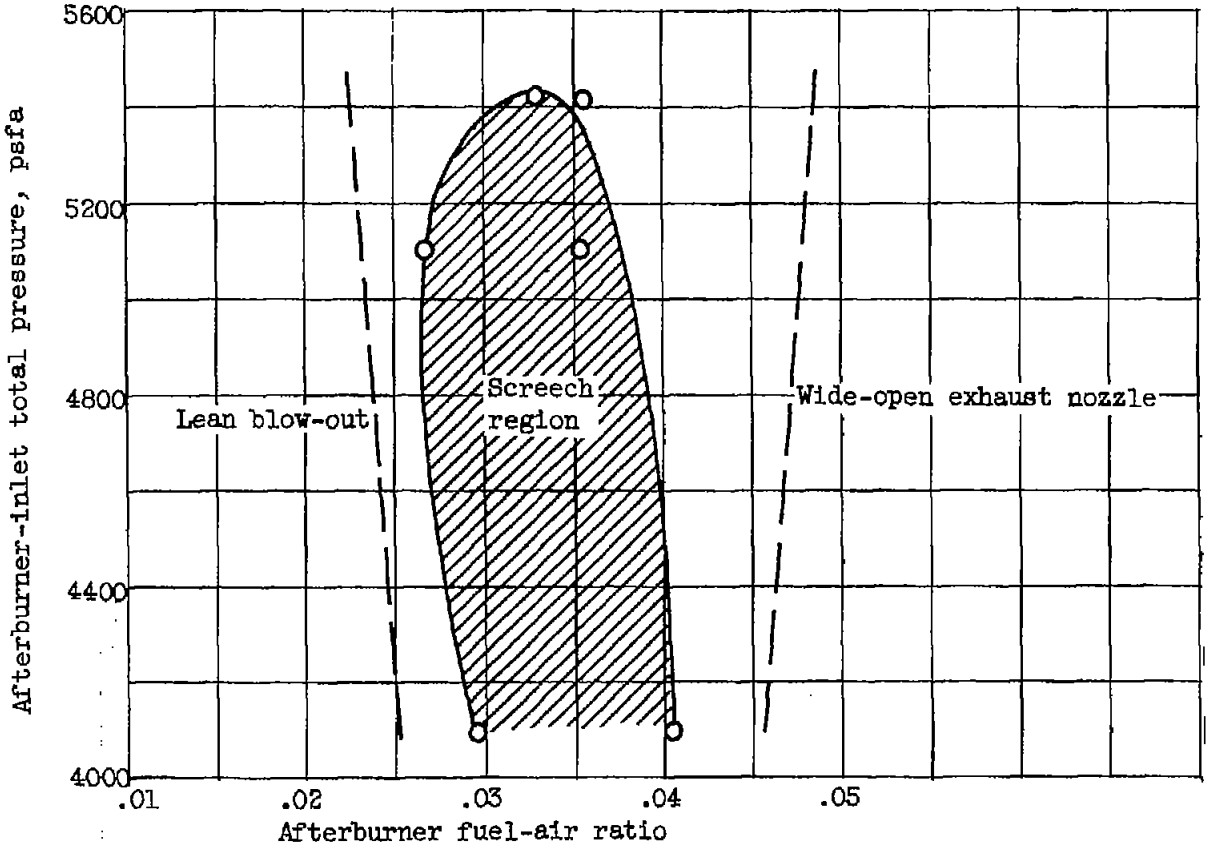

(b) Configuration 8.

Figure 12. - Concluded. Effect of pressure and fuel-air ratio on screech boundaries.

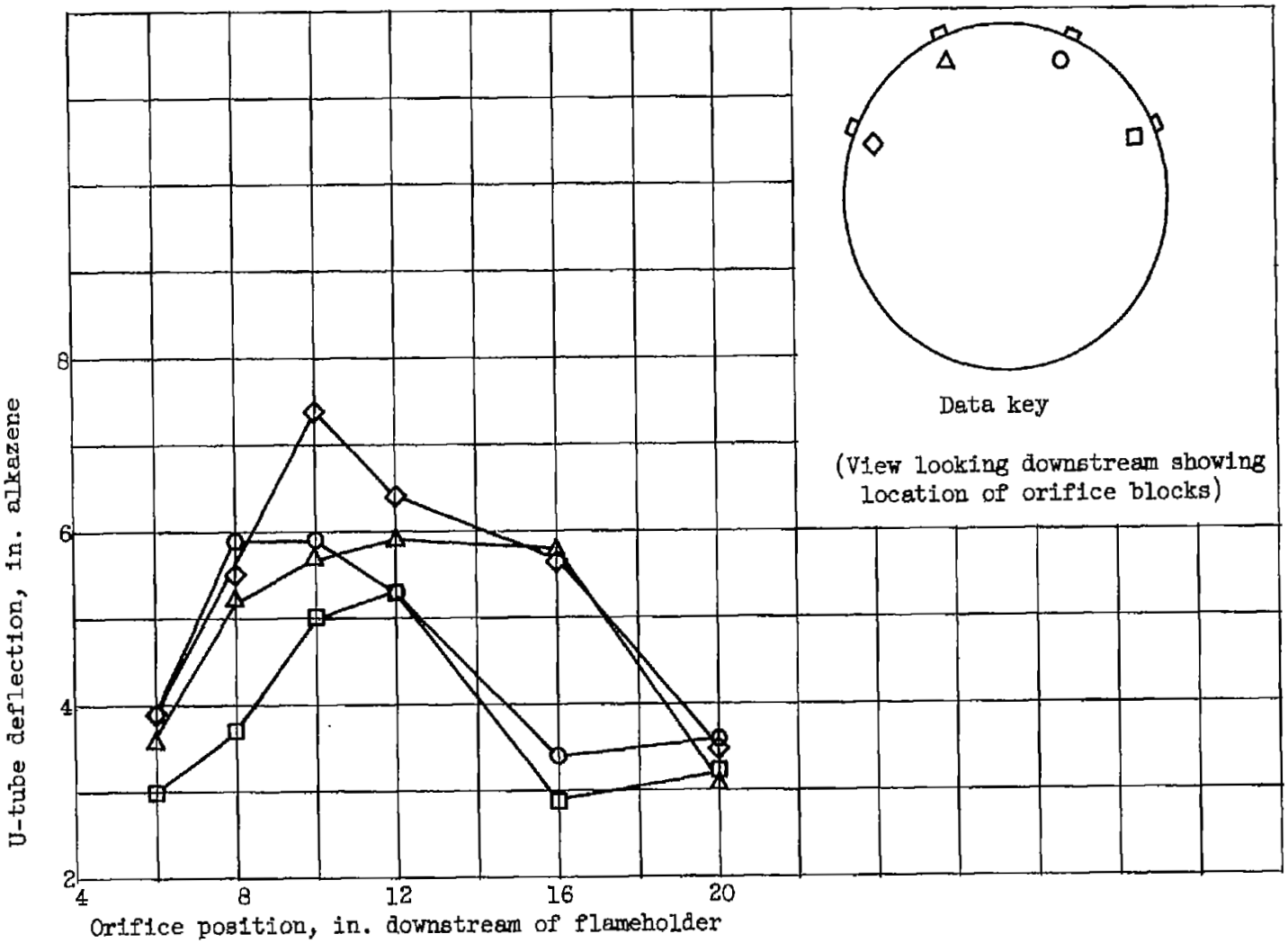

Figure 13. - Typical screech-induced deflection pattern in U-tube manometers connected to differential pressure orifices (configuration 23).